URA3 nutritional selection), enabling the construction of simple readout assay systems.

Gag protein, the main structural component of retrovirus, directs particle assembly. HIV Gag protein is synthesized as a precursor protein, p55, which is composed of matrix (MA), capsid (CA), nucleocapsid (NC), and p6 domains, and cotranslationally myristoylated at the N-terminal glycine. Concomitant with the N-terminal myristoylation, p55Gag is targeted to the plasma membrane and assembled into virus particles (13, 22). During particle release, Gag undergoes proteolytic processing to generate the CA domain that forms the mature capsid. In the next round of infection, the mature capsid disassembles during viral penetration into host cell cytoplasm. Thus, the capsid assembly and disassembly are reverse reactions during virus release and entry and must be regulated by yet-unknown mechanisms. Indeed, the optimal stability of HIV-1 capsid is required for efficient infection (14). We have previously shown that the particle assembly process is reproducible in a yeast cell system (26). Here, we further developed a yeast membrane-associated two-hybrid assay system in which a temperature-sensitive mutant strain of yeast grows at restrictive temperature when Gag-Gag interactions occur. Using this yeast two-hybrid system, we have screened a chemical library composed of 20,000 low-molecular-weight compounds and have found a compound that targets CA-CA interactions and inhibits HIV-1 replication.

MATERIALS AND METHODS

Construction and transformation of yeast expression plasmids. A yeast membrane-associated two-hybrid assay based on the CytoTrap SOS recruitment system (Stratagene) was employed in this study. The full-length *gag* gene of HIV-1 (HXB2 strain) was placed downstream of the yeast inducible promoter for the *GAL1* gene in frame with the cDNA of SOS in a pSOS plasmid (Stratagene) that contains the *LEU2* gene as a yeast selective marker. The HIV-1 (HXB2 strain) *gag* gene was also cloned into pMyr plasmid, which contains a yeast inducible promoter for the *GAL1* gene and the *URA3* gene as a selective marker. The *S. cerevisiae* strain cdc25Ha (*MAT*a *ura3-52 his3-200 ade2-101 lys2-801 trp1-901 leu2-3 112 cdc25-2* Gal$^+$) was doubly transformed with the yeast expression plasmids.

Chemical library screening in CytoTrap yeast membrane-associated two-hybrid system. Yeast transformants were initially grown at 25°C in synthetic defined medium with glucose (0.67% yeast nitrogen base, 2% glucose, and amino acid mixtures without uracil or leucine) (permissive conditions). After being washed, culture was diluted to an optical density at 600 nm (OD_{600}) of 0.1 in synthetic defined medium with galactose and raffinose (0.67% yeast nitrogen base, 2% galactose, 2% raffinose, and amino acid mixtures without uracil or leucine) for Gag expression. The yeast culture (OD_{600} = 0.1) was incubated with a chemical library (a final concentration of 10 μM) at 37°C for 5 days (restrictive conditions) in 96-well microtiter plates with shaking. The chemical library (preplated Diversity Set) was purchased from Enamine. After complete resuspension of cells by vortexing of microtiter plates, cell density was measured at 600 nm by a plate reader (Infinite200; Tecan).

Mammalian cells and transfection. 293T, HeLa, and MT-4 cells were provided by the AIDS Research Center, National Institute of Infectious Diseases, Japan. 293FT cells were purchased from Invitrogen. Peripheral blood monocytic cells (PBMC) were isolated by Ficoll-Conray density centrifugation from healthy donors. All mammalian cells were maintained in RPMI 1640 medium (Sigma) supplemented with 10% fetal bovine serum (Japan Bioserum, Japan), 100 U/ml penicillin, and 100 mg/ml streptomycin (Invitrogen), at 37°C in a humidified 5% CO_2 atmosphere. For PBMC culture, GlutaMax-I (Invitrogen), insulin-transferrin-selenium A (Invitrogen), 200 ng/ml anti-CD3 monoclonal antibody (OKT3; Janssen Pharmaceutical), and 70 U/ml recombinant human interleukin-2 (IL-2; Shionogi Pharmaceutical, Japan) were further added to the medium. Transfection was carried out with Lipofectamine 2000 according to the manufacturer's protocol (Invitrogen).

Cell toxicity assays. For determining the toxicity of the chemical library to yeast, yeast cultures were diluted to an OD_{600} of 0.01 and incubated under permissive conditions (at 25°C in glucose medium) with the chemical library. After 2 days, cell density was measured at 600 nm by a plate reader (Infinite200; Tecan). For determining toxicity to mammalian cells, 293T, 293FT, HeLa, and MT-4 cells and PBMC were incubated with compounds at 37°C for 2 to 14 days and subjected to 3-(4,5-dimethylthiazol-2-yl)-5-(3-carboxymethoxyphenyl)-2-(4-sulfophenyl)-2H-tetrazolium (MTS) and Alamar Blue assays according to the manufacturer's instructions. The OD of the MTS assay mixture was measured at 490 nm, and the OD of the Alamar Blue assay mixture was measured at 570 nm by a plate reader (FLx800; BioTek). The 50% cytotoxicity concentrations were defined as drug concentrations by which the OD values reached the 50% level of the no-drug (dimethyl sulfoxide [DMSO]) controls.

HIV-1 replication assays. MT-4 Luc cells that were transduced with luciferase in MT-4 cells (31) and PBMC were grown in RPMI 1640 medium supplemented with 10% fetal bovine serum. MT-4 Luc cells were infected with HIV-1 (HXB2 strain) corresponding to 1.25 ng of p24CA antigen and incubated at 37°C in the presence of compounds. On day 7, MT-4 Luc cells were subjected to luciferase assay. PBMC were stimulated with IL-2 and anti-CD3 antibody. Following infection with HIV-1 (HXB2 strain) corresponding to approximately 5 ng of p24CA antigen, PBMC were incubated at 37°C and passaged every 3 to 4 days in the presence of compounds. The culture supernatants of PBMC were temporally collected and subjected to quantification of HIV-1 particle yields by p24CA antigen capture enzyme-linked immunosorbent assay (ELISA; Zeptometrix).

Single-round infection assays. For single-round infection assays, HIV-1 was pseudotyped with either HIV-1 Env protein or vesicular stomatitis virus (VSV) G protein as described previously (35). Briefly, 293FT cells were transfected with a plasmid containing the codon-optimized HXB2 *gag-pol* gene (pHIVgag-pol), a lentiviral plasmid expressing luciferase (pLenti-luciferase), a plasmid expressing HIV-1 Rev (pRevpac), and either a plasmid expressing HIV-1 Env or a plasmid expressing VSV-G. Culture media were harvested and inoculated into MT-4 and 293FT cells in the presence of 5 to 10 μg/ml dextran (ICN). HIV-1 pseudotyped with autologous HIV-1 Env protein was inoculated into 293FT-CD4 (expressing CD4 constitutively) cells. On day 2 or 3, infectivity was assessed by luciferase activity transduced by pLenti-luciferase. HIV-1 (NL43 strain) expressing luciferase, simian immunodeficiency virus (SIV) (mac239 strain), and murine leukemia virus (MLV) (Moloney strain) were similarly pseudotyped with VSV-G (28). The viruses were enriched by centrifugation through sucrose cushions if necessary.

HIV/SIV Gag chimeras were generated in the context of pHIVgag-pol by replacing the MA and CA domains with the SIV MA and CA domains, respectively. The Gag chimeras contain the cleavage site sequences of HIV-1 Gag at the chimera junctions. Amino acid substitutions G89A and P90A in the cyclophilin A (CypA)-binding loop of CA (corresponding to Gag amino acid positions 225 and 226) (11, 16) were carried out by overlap PCR in the context of pHIVgag-pol.

Quantitative PCR for HIV-1 cDNA synthesis. MT-4 cells were infected with HIV-1 (HXB2 strain) and incubated in the presence of compounds. Efavirenz (EFV) was provided by the NIH AIDS Research and Reference Reagent Program and was used as positive control. The cellular genomic DNA was extracted 4 and 24 h postinfection with a DNeasy kit (Qiagen) according to the manufacturer's instructions. The cellular DNA was subjected to quantitative real-time PCR using the Quantitec probe PCR kit containing SYBR green (Qiagen). The following primer sets were used: 5′-AACTAGGGAACCCACTGCTTAAG-3′ and 5′-CTGCTAGAGATTTTCCACACTGAC-3′ (specific for the R-U5 region in early reverse transcripts of HIV-1 cDNA), 5′-CCGTCTGTTGTGTGACTC TGGT-3′ and 5′-GAGTCCTGCGTCGAGAGAGCT-3′ (specific for the late reverse transcripts of HIV-1 cDNA), 5′-TGCTGGGATTACAGGCGTGAG-3′ and 5′-CTGCTAGAGATTTTCCACACTGAC-3′ (specific for long terminal repeat [LTR] and *Alu* region in the integrated HIV-1 cDNA), and 5′-AACTAG GGAACCCACTGCTTAAG-3′ and 5′-CTGCTAGAGATTTTCCACACTGA C-3′ (second PCR) (specific for LTR region in the integrated HIV-1 cDNA) (12). The amplification kinetics was monitored by the Opticon 2 system (Bio-Rad). The levels of cellular DNA were normalized by the levels of β-globin DNA quantified using primers 5′-TATTGGTCTCCTTAAACCTGTCTTG-3′ and 5′-CTGACACAACTGTGTTCACTAGC-3′ (19).

Viral protein expression and particle purification. HIV-1 proviral clone pHXB2 was transfected into 293FT and HeLa cells in the presence of increasing doses of 2-(benzothiazol-2-ylmethylthio)-4-methylpyrimidine (BMMP). After 2 days, cells were analyzed by Western blotting using anti-HIV-1 p24CA monoclonal antibody (100-fold diluent of 183-H12-5C hybridoma culture supernatant; NIH AIDS Research and Reference Reagent Program). HIV particles were collected by centrifugation through 20% (wt/vol) sucrose cushions in an SW55

rotor (Beckman Coulter) at 120,000 × *g* for 1 h. For HIV/SIV Gag chimeras, 293FT cells were cotransfected with pHIVgag-pol expressing Gag chimera, pLenti-luciferase, pRevpac, and a plasmid expressing VSV-G. Cells and purified particles were similarly analyzed by Western blotting using anti-HIV-1 p24CA, anti-HIV-1 p17MA (2 μg/ml; 13-103-100; Advanced Biotechologies), and anti-SIV p27CA (1 μg/ml; 4324; Advanced Bioscience Laboratories) monoclonal antibodies.

***In vitro* assembly reaction of CA.** The *in vitro* assembly reaction of CA was performed as described previously (17, 36). Briefly, the purified HIV-1 CA (a final concentration of 100 μM) was incubated at 37°C for 1 h in buffer containing 20 mM Tris (pH 8.0), 500 mM NaCl, 0.2 mM EDTA, and 1 mM dithiothreitol. Assembly products were pelleted by centrifugation at 18,000 × *g* for 30 min at 4°C and were subjected to p24CA antigen capture ELISA (Zeptometrix) and electron microscopy.

***In vitro* disassembly reaction of capsid cores.** The *in vitro* disassembly assay was performed according to Aiken's method with some modifications (3). HIV particles were purified by ultracentrifugation through 20% (wt/vol) sucrose cushions. For isolation of HIV capsid cores, purified HIV particles were applied onto sucrose step gradients composed of 7.5% (wt/vol), 15% (wt/vol) containing 1% Triton X-100, and 30 to 70% (wt/vol) sucrose and subjected to centrifugation at 120,000 × *g* for 16 h at 4°C. Fractions rich in HIV cores were collected and resuspended in buffer (10 mM Tris [pH 7.4], 100 mM NaCl, and 1 mM EDTA). For core disassembly assays, aliquots of HIV cores were incubated at 37°C in the presence of compounds. For comparison, azidothymidine (AZT) (Moravek Biochemicals) was added to the reaction mixture. Intact cores were recovered by centrifugation at 125,000 × *g* for 30 min at 4°C.

Confocal microscopy and electron microscopy. HeLa cells were transfected with a pNL43 derivative expressing Gag-green fluorescent protein (GFP) fusion protein but not *pol* gene products. Cells were fixed with 3.7% paraformaldehyde in phosphate-buffered saline (PBS) for 30 min at room temperature and were treated with 0.1% Triton X-100 for 10 min at room temperature for membrane permeabilization. Following nuclear staining with TO-PRO-3 (Molecular Probes), cells were mounted with antibleaching reagent and observed with a laser scanning microscope (TCS; Leica).

In vitro assembly products were adsorbed onto carbon-coated copper grids and stained with 2% (wt/vol) uranyl acetate. Sections were subjected to electron microscopy.

Statistical analysis. Intergroup comparisons were performed with paired *t* test (for parametric group analysis). All *P* values were considered significant if less than 0.05.

RESULTS

A yeast membrane-associated two-hybrid system for HIV-1 Gag-Gag interactions. For construction of a yeast cell-based Gag assembly system, we employed a yeast membrane-associated two-hybrid assay based on the CytoTrap SOS recruitment system (Stratagene) in this study (Fig. 1). For HIV-1 Gag expression, two yeast expression plasmids, pMyr and pSOS, were used: pMyr contains the yeast inducible promoter for the *GAL1* gene followed by a myristoylation signal (amino acid sequence, MGSSKSKPKDPSQRR) for membrane targeting and pSOS contains the constitutive promoter for the yeast *ADH* gene followed by the human SOS gene. The *gag* gene of HIV-1 (HXB2 strain) was cloned in frame with the myristoylation signal in pMyr. The *gag* gene was similarly cloned in frame with the SOS gene in pSOS that allowed production of SOS-Gag fusion protein (Fig. 1A). The *S. cerevisiae* cdc25H strain was doubly transformed with these Gag expression plasmids. The cdc25H strain contains a temperature-sensitive mutation in the CDC25 gene, which allows growth at 25°C (permissive temperature) but not at 37°C (restrictive temperature). SOS is the human orthologue of the yeast CDC25 and can activate the yeast RAS signal transduction pathway that complements the yeast *cdc25* defect (4). When myristoylated Gag and SOS-Gag are coexpressed in the cdc25H cells, the SOS-Gag is recruited to the plasma membrane through an interaction with the myristoylated Gag, leading to growth of the cdc25H cells at 37°C (Fig. 1B). We initially confirmed that the cdc25H cells transformed with the Gag/pMyr and Gag/pSOS plasmids grew at 37°C in galactose plus raffinose medium under conditions in which SOS-Gag fusion protein was expressed but not at 37°C in glucose medium under conditions in which SOS-Gag fusion was not expressed.

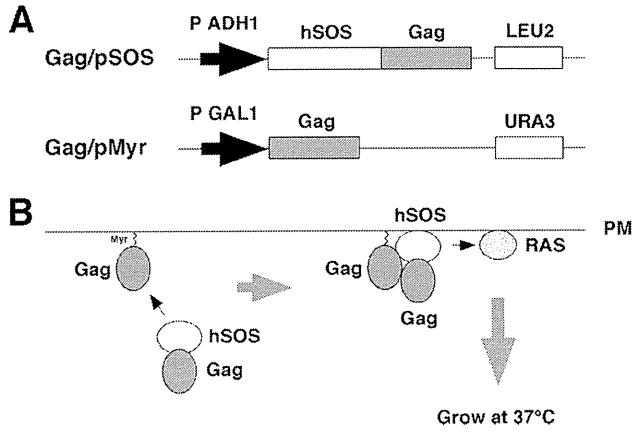

FIG. 1. Yeast membrane-associated two-hybrid screening for inhibitors of Gag-Gag interaction. (A) Schematic representation of Gag expression plasmids used for yeast SOS recruitment system. The full-length *gag* gene of HIV-1 (HXB2 strain) was expressed by yeast expression plasmids pMyr and pSOS: pMyr contains the yeast inducible promoter for the *GAL1* gene and the *URA3* gene as a selective marker and pSOS contains the constitutive promoter for the yeast *ADH* gene and the *LEU2* gene as a selective marker. (B) Principle of yeast membrane-associated two-hybrid assay based on SOS recruitment system. The schematic illustration was adapted with permission from the manuals for the CytoTrap yeast system (Agilent Technologies, Inc.; http://www.genomics.agilent.com/CollectionSubpage.aspx?PageType=Product&SubPageType=ProductDetail&PageID=1311).

Screening of a chemical library for Gag-Gag interaction inhibitors by yeast membrane-associated two-hybrid assays. For screening for inhibitors of Gag assembly, we optimized this yeast membrane-associated Gag-Gag interaction system to a liquid format using 96-well microplates. Using this system, we screened a chemical library composed of 20,000 compounds, each of which was initially designated by the numbers of microplates and wells of the chemical library (e.g., 172A6 indicates microplate number 172 and well number A6). When the cdc25H transformant was incubated at 37°C in galactose plus raffinose medium with a chemical library (10 μM each), we found 10 compounds that reduced cell growth (Fig. 2A, black columns). To examine if cell growth reduction is specifically due to the disruption of Gag-Gag interaction, we used another cdc25H transformant that contained MAFB/pSOS and SOS binding protein/pMyr plasmids. This combination produces SOS-MAFB fusion protein and myristoylated SOS binding protein and can be used as a positive control for the CytoTrap system (Stratagene). When using this positive control, we observed that 4 compounds (2G5, 73A7, 189A9, and 235C2) out of the 10 compounds also reduced cell growth (Fig. 2A, white columns), suggesting that they might inhibit pathways which are commonly used in the CytoTrap system (e.g., N myristoylation and RAS signaling). Thus, we concluded that 6 compounds (1G5, 31E7, 34A8, 73A5, 147B2, and 172A6) specifi-

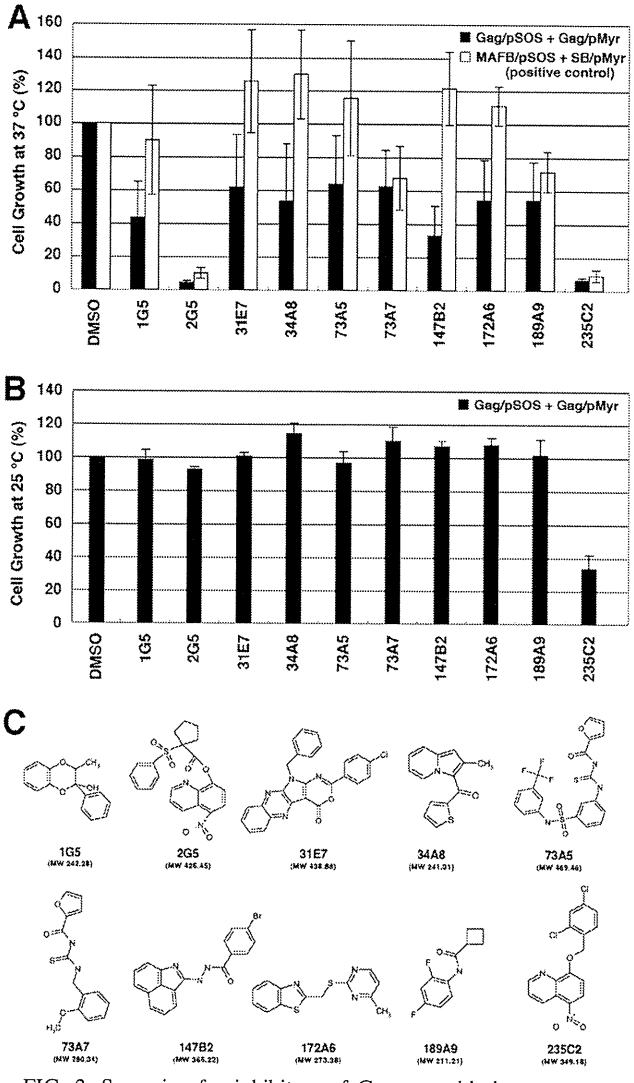

FIG. 2. Screening for inhibitors of Gag assembly by yeast membrane-associated two-hybrid assays. (A) The yeast cdc25Ha strain was transformed with the pSOS and pMyr plasmids. The yeast culture was diluted to an OD_{600} of 0.1 and incubated at 37°C in galactose-plus-raffinose medium (restrictive conditions) with a chemical library (a final concentration of 10 μM). After growth at 37°C for 5 days, cell density was measured at OD_{600}. As a control, the OD_{600} of yeast incubated in the presence of DMSO was set to 100%. The yeast transformed with the pSOS and pMyr plasmids, both of which contained the HIV-1 *gag* gene, was shown as black columns, and the yeast was transformed with the pSOS plasmid containing MAFB and the pMyr plasmid containing the cDNA of SB (as a positive-control combination) as white columns. Data were shown as means with standard deviations from 5 independent experiments. (B) The yeast cdc25Ha strain transformed with the pSOS and pMyr plasmids containing the HIV-1 *gag* gene was grown at 25°C in glucose medium. The yeast culture was diluted to an OD_{600} of 0.01 and incubated at 25°C in glucose medium with a chemical library (a final concentration of 10 μM). After growth at 25°C for 2 days, cell density was measured at OD_{600}. As a control, the OD_{600} of yeast incubated in the presence of DMSO was set to 100%. Data were shown as means with standard deviations from 3 independent experiments. (C) Structures of compounds screened from a chemical library by yeast membrane-associated two-hybrid assays.

cally inhibited a Gag-Gag interaction. No common chemical structures were found among the 6 candidates. However, 3 chemicals (34A8, 147B2, and 172A6) share relatively similar structures whereby two allyl groups are connected by a short linker moiety. To test the cell toxicity, the cdc25H transformants were incubated at 25°C in glucose medium (permissive conditions) with the compounds (10 μM each) (Fig. 2B). All the compounds except 235C2 allowed cell growth at levels comparable to that obtained in the presence of DMSO (as a control). Further studies revealed that 235C2 preferentially inhibited growth of several fungi *in vitro* (e.g., *Candida albicans* and *Aspergillus fumigatus* at MICs of 5.7 and 10 μM, respectively) (data not shown), suggesting that it might serve as a lead compound to develop an antifungal agent. The chemical formulas of 10 compounds are shown in Fig. 2C.

Inhibition of HIV replication in mammalian cells by compounds identified as yeast membrane-associated Gag-Gag interaction inhibitors. We evaluated the anti-HIV activity of the 6 candidates in mammalian cell systems. MT-4 Luc cells (human T lymphocytic cell line expressing luciferase constitutively) were infected with HIV-1 (HXB2 strain) and incubated at 37°C in the presence of the test compounds. In this T cell system, the luciferase activity is reduced by HIV-1 infection, due to the cell death upon HIV-1 replication (31). When added to HIV-1-infected MT-4 Luc cells, one of the candidates (172A6) recovered the luciferase expression in a dose-dependent manner (Fig. 3A), indicating that 172A6 was capable of reduction in HIV replication in mammalian cells. When 293T cells were incubated with the 6 compounds and were subjected to Alamar Blue assays, none of the compounds showed apparent reduction in cell viability (Fig. 3B). To confirm the anti-HIV effect, PBMC were infected with HIV-1 in the presence of 172A6 and production of HIV in the culture medium was temporally measured by p24CA antigen capture ELISA. 172A6 limited HIV replication at 5 μM and severely inhibited it at 25 μM (Fig. 3C, upper panel). When uninfected PBMC were similarly exposed to 172A6 and assessed by MTS assays, a slight reduction in cell viability was observed at 25 μM (Fig. 3C, lower panel). However, the severe inhibition of HIV replication at 25 μM 172A6 could not be ascribed fully to its cytotoxic effect. Using several mammalian cell lines, we reevaluated cytotoxicity of 172A6 by MTS assays. No significant cytotoxicity of 172A6 was seen in the cell lines, except in PBMC, that we used in this study (Fig. 3D). Based on the chemical structure [2-(benzothiazol-2-ylmethylthio)-4-methylpyrimidine] of the compound 172A6 (Fig. 2C), we called it BMMP here.

No inhibition of HIV particle release by BMMP. We initially examined whether BMMP inhibited HIV-1 particle production. 293FT cells were transfected with pHXB2 and incubated at 37°C in the presence of 5 to 50 μM BMMP. Western blotting using anti-HIV-1 p24CA antibody revealed that the intracellular level of Gag expression and the pattern of Gag processing were largely unaffected in the presence of BMMP (Fig. 4A), suggesting that BMMP did not inhibit HIV protease. When purified particle fractions were similarly analyzed, we found no reduction in particle production (Fig. 4A). We obtained similar results on HeLa cells. This indicates that BMMP did not block HIV-1 particle release.

Intracellular distribution of Gag was examined by confocal

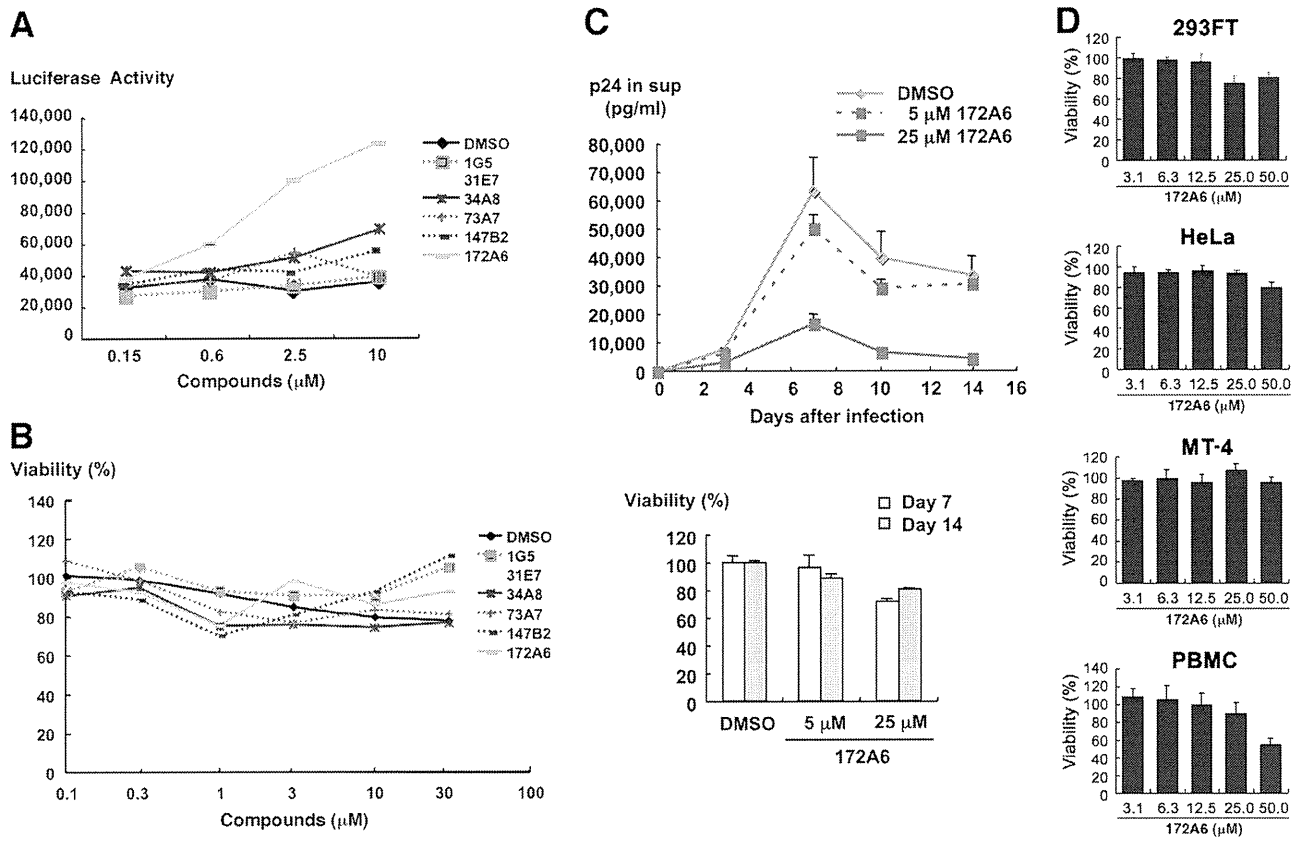

FIG. 3. Inhibition of HIV-1 replication and cell toxicity. (A) MT-4 Luc cells were infected with HIV-1 (HXB2 strain) and incubated at 37°C in the presence of increasing doses of compounds. On day 7, MT-4 Luc cells were subjected to luciferase assay. Data were shown as means from triplicate cultures. (B) 293T cells were incubated with various doses of compounds at 37°C for 2 days and subjected to Alamar Blue assays. Data were shown as means from 3 independent experiments. (C) PBMC stimulated with IL-2 and anti-CD3 antibody were infected with HIV-1 (HXB2 strain) and incubated at 37°C in the presence of 5 and 25 μM 172A6. HIV-1 production in culture medium was temporally quantified by p24CA antigen capture ELISA (top). Uninfected PBMC were cultured with 172A6 at 37°C and were subjected to MTS assay on days 7 and 14. Data were shown as means with standard deviations from triplicate cultures, in which DMSO was used as control. (D) 293FT, HeLa, and MT-4 cells and PBMC were incubated at 37°C with various doses of 172A6 and were subjected to MTS assay on days 4, 3, 4, and 6, respectively. Cell viability was shown as OD_{490}. Data were shown as means with standard deviations from triplicate cultures.

microscopy (Fig. 4B). HeLa cells were transfected with a pNL43 derivative that expresses Gag-GFP and incubated with 30 μM BMMP. Gag-GFP was distributed predominantly at the plasma membrane in cells treated with DMSO (used as control). A similar Gag-GFP distribution was observed in cells treated with BMMP, indicating that BMMP did not inhibit Gag targeting to the plasma membrane, consistent with the above findings.

Inhibition of HIV replication postentry by BMMP. To examine whether BMMP exerted an inhibitory effect on early stages of the HIV life cycle, such as viral entry, we employed single-round infection assays with luciferase-expressing HIV-1 vectors which were pseudotyped with either VSV-G or authentic HIV-1 Env protein. To this end, pHIVgag-pol (for expression of HIV-1 Gag and Gag-Pol), pRevpac (for expression of HIV-1 Rev), and pLenti-luciferase vector, which provides the artificial lentiviral genome expressing luciferase driven by cytomegalovirus promoter, were cotransfected with either VSV-G or authentic HIV-1 Env expression plasmid into 293FT cells. HIV-1 Luc viruses produced were inoculated into MT-4 cells in the presence of BMMP, and viral infectivity was monitored by a luciferase reporter assay. Luciferase expression was inhibited in a BMMP dose-dependent manner in cells infected with the HIV-1 Env-pseudotyped Luc virus, indicating that BMMP inhibited the early stage of the HIV-1 life cycle (Fig. 5A). However, when VSV-G-pseudotyped Luc virus was used, a dose-dependent reduction was similarly observed. When HIV-1 (NL43 strain) expressing luciferase was pseudotyped with VSV-G and used in this assay, the luciferase activity driven by the LTR promoter was similarly reduced in the presence of BMMP, suggesting that BMMP did not inhibit the stage of HIV entry (e.g., attachment and membrane fusion processes) but the stage of postentry (e.g., uncoating) (Fig. 5A). The Env-independent infectivity reduction was confirmed when HIV-1 Luc viruses were inoculated into 293FT and 293FT-CD4 cells (Fig. 5B). We examined whether BMMP also blocked the postentry stage of SIV. Interestingly, single-round infection assays with luciferase-expressing SIVmac239 vectors which were pseudotyped with VSV-G protein showed no inhibition of luciferase expres-

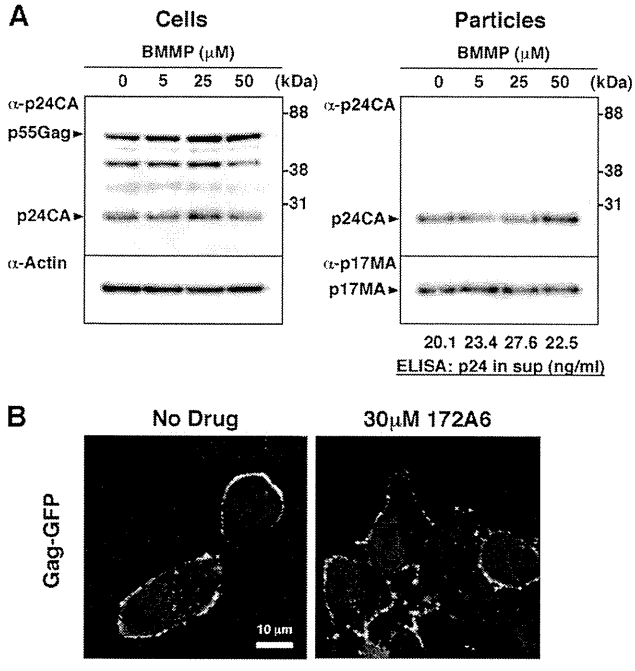

FIG. 4. HIV-1 particle production and Gag plasma membrane targeting. (A) Effects on HIV-1 particle production. 293FT cells were transfected with pHXB2 and incubated at 37°C with 0 to 50 μM BMMP. Two days posttransfection, cells were collected and culture media were subjected to purification of viral particles by ultracentrifugation. Equivalent volumes of samples were subjected to SDS-PAGE followed by Western blotting using anti-HIV-1 p24CA antibody. Representative blots were shown. HIV-1 particle yields in culture media were quantified by p24CA antigen capture ELISA. (B) Intracellular localization of Gag. HeLa cells were transfected with a pNL43 derivative in which Gag was fused with GFP and incubated at 37°C for 1.5 days with 30 μM BMMP. Nuclei were stained with TO-PRO-3, and cells were observed by confocal microscopy. Representative images were shown at the same magnification. Bar = 10 μm.

sion (Fig. 5B). No reduction in luciferase expression was also observed when luciferase-expressing pseudotyped MLV was used (data not shown). These data suggest that BMMP specifically inhibits HIV replication postentry but not those of other retroviruses, such as SIV and MLV.

To confirm the postentry block prior to particle production, we isolated cellular DNA from MT-4 cells infected with HIV-1 (HXB2 strain) that were treated with BMMP. Then, we quantified early reverse transcripts of HIV (corresponding to the strong-stop DNA), late reverse transcripts of HIV, and integrated HIV DNA by PCR. When normalized to the level of β-globin DNA (internal control), the levels of the early and late reverse transcripts and of the integrated proviral DNA were reduced, as observed for cells treated with 200 nM efavirenz controls (Fig. 5C). However, RT enzymatic activity was not affected by BMMP when examined in *in vitro* assays (data not shown). Together, these data indicate that BMMP blocks the early stage of the HIV-1 life cycle, preventing the completion of reverse transcription.

Mapping of Gag domain targeted by BMMP. To map the HIV Gag domain responsible for the postentry block by BMMP, a series of chimeric Gag constructs between HIV-1 and SIVmac239 were made in the context of pHIVgag-pol. HIV-1 MA, MACA, and CA were replaced by SIV MA, MACA, and CA, respectively (referred to as sMA, sMACA, and sCA, respectively). These Gag/Gag-Pol expression plasmids were cotransfected with pRevpac and pLenti-luciferase vector, and viruses were pseudotyped with VSV-G protein. Western blotting using anti-HIV-1 p17MA and p24CA and anti-SIVmac p27CA antibodies revealed that, although the anti-HIV-1 p24CA antibody that we used was cross-reactive with SIV CA, each domain of Gag was replaced in the chimeric constructs and virus particles were produced at levels largely similar to that of the wild type of HIV-1 Gag construct (Fig. 6A). Single-round infection assays with these Gag chimeras revealed that BMMP inhibited viral infection postentry only when HIV-1 CA was present in the constructs (Fig. 6B). Thus, our data indicated that BMMP inhibited the early stage of HIV-1 replication in a CA-specific and species-specific manner. These phenotypes resemble those observed for the CA-specific retroviral restriction imposed by a host factor, tripartite motif protein 5 (TRIM5) (30). HIV-1 CA is known to bind a host factor, CypA, likely through amino acids G89 and P90 in the exposed loop of CA (15, 16). This binding facilitates the early stage of HIV-1 replication prior to reverse transcription (9). Interestingly, HIV/SIV chimera studies have shown that the CypA-binding site overlaps with the determinants for species-specific restriction (30, 34). Thus, we made an HIV-1 Gag construct containing amino acid substitutions G89A and P90A in the CypA-binding loop of CA (referred to as CypA mt) and tested the sensitivity to BMMP. The CypA mt did not display the resistance to BMMP (Fig. 6B), suggesting that HIV-1 inhibition by BMMP was not linked to the CypA binding or TRIM5. No firm conclusions were drawn from mapping experiments using Gag chimeras within CA, i.e., N- and C-terminal domains (NTD and CTD), since the CTD mutant showed a lower yield of particle production (data not shown).

Disassembly of HIV capsid core by BMMP. The chimera experiments showed that the CA domain is critical for the inhibitory effect of BMMP on the early stage of HIV-1 replication. Thus, we examined whether BMMP affects CA-CA interaction using purified CA. An *in vitro* assembly reaction with purified HIV-1 CA was employed to test if BMMP disrupted CA-CA interactions. *In vitro* assembly reaction of CA has shown it to produce tubular structures representing the mature CA capsid structure (17, 36). We added BMMP to the *in vitro* assembly reaction with 100 μM HIV-1 CA, and resultant CA assembly products were observed by electron microscopy (Fig. 7A). For quantitative analysis, the resultant CA assembly products were recovered by ultracentrifugation and subjected to SDS-PAGE. The levels of the CA assembly products were reduced when BMMP was added at a concentration higher than 30 μM, corresponding to approximately a 1:3 molar ratio to CA (Fig. 7A). These data suggest that BMMP targets HIV-1 CA and leads to the destabilization of the viral capsid core, since our previous findings indicated that BMMP did not block particle release (Fig. 4) but did block the HIV-1 infection postentry (Fig. 5).

To test this possibility in a more relevant assay, we adopted cell-free disassembly assays using purified HIV-1 mature capsid core. To this end, we isolated HIV-1 capsid cores by ultracentrifugation through a Triton X-100 layer, as described pre-

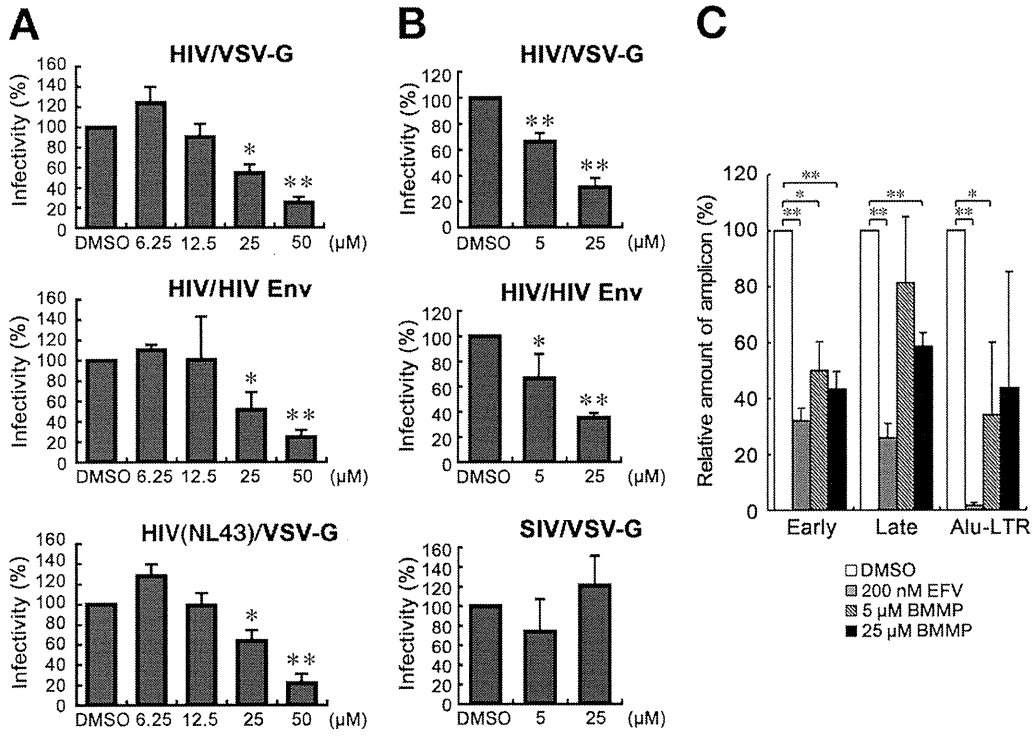

FIG. 5. Inhibition of HIV-1 replication postentry. (A) Single-round infection assays in MT-4 cells. 293FT cells were cotransfected with pHIVgag-pol (derived from HXB2 strain), pLenti-luciferase, pRevpac, and either a plasmid expressing HIV-1 Env (middle) or a plasmid expressing VSV-G (top). HIV-1 (NL43 strain) expressing luciferase was similarly pseudotyped with VSV-G protein (bottom). Following incubation, the culture supernatants were recovered and were subsequently inoculated into MT-4 cells with increasing doses of BMMP. (B) Single-round infection assays in 293FT and 293FT-CD4 cells. HIV-1 vectors containing the luciferase gene were similarly pseudotyped with HIV-1 Env (middle) or VSV-G protein (top). Luciferase-expressing SIVmac was pseudotyped with VSV-G protein by cotransfection (bottom). Viruses produced were subsequently inoculated into 293FT (top and bottom) or 293FT-CD4 (middle) cells with 5 and 25 μM BMMP. Viral infectivity was assessed by luciferase reporter assays. Data were shown as means with standard deviations from 3 to 6 independent experiments in panels A and B. *, $P < 0.05$; **, $P < 0.01$. (C) Quantitative PCR. MT-4 cells were infected with HIV-1 (HXB2 strain) and incubated in the presence of BMMP. DNA was isolated at 4 or 24 h postinfection and subjected to quantitative PCR for HIV cDNA. Reverse transcripts generated at the early and late phases of HIV reverse transcription were amplified from the DNA isolated at 4 and 24 h postinfection, respectively. The integrated viral genome was amplified as *Alu*-LTR transcripts from the DNA isolated at 24 h postinfection. EFV (200 nM) was used as positive controls. Three independent infections were performed, and quantitative PCR was carried out in triplicate with each infection sample. Representative data were shown with the means and standard deviations. *, $P < 0.05$; **, $P < 0.01$.

viously (3). HIV-1 cores are known to disassemble when incubated at 37°C. We examined if BMMP accelerated the rate of core disassembly. The HIV-1 cores were incubated with BMMP at 37°C up to 120 min, and residual intact cores were recovered by centrifugation. When quantified by p24CA antigen capture ELISA, intact cores were found to be reduced in a time-dependent manner in the presence of DMSO (as control), consistent with previous reports (3). A similar level of reduction was observed in the presence of AZT. However, addition of BMMP accelerated a reduction in intact cores in a dose-dependent manner (Fig. 7B). Altogether, our data indicated that BMMP disrupted HIV-1 capsid cores through targeting CA.

DISCUSSION

In this study, we employed a yeast membrane-associated two-hybrid assay to monitor the HIV Gag-Gag interactions and established cell-based screening assays for drugs targeting Gag assembly. We screened a commercially available chemical library and found BMMP, which inhibits HIV-1 replication in PBMC culture. Our single-round infection analysis indicated that BMMP primarily targets HIV-1 CA and inhibits HIV infection postentry but not particle production (Fig. 4 to 6). *In vitro* CA assembly/disassembly assays showed that BMMP facilitated HIV-1 core disassembly (Fig. 7). Collectively, it is conceivable that BMMP may bind to mature capsid structure and facilitate disassembly of the capsid, leading to premature earlier uncoating and failure of postentry events (e.g., reverse transcription and integration). The mechanism of action may be akin to the block of HIV-1 entry by rTRIM5α (30).

Previous studies have reported inhibitors that target HIV-1 Gag assembly and/or Gag processing. 3-*O*-(3′,3′-Dimethylsuccinyl)betulinic acid, known as PA-457 or Bevirimat (molecular weight, 584), binds to the Gag CA-SP1 cleavage site and inhibits proteolytic conversion of Gag precursors to the mature form of p24CA (50% inhibitory concentration [IC_{50}] = 10 nM) (1, 2, 21). Inhibition of Gag processing has also been observed with a distinct chemical class of compound, 1-[2-(4-tert-butylphenyl)-2-(2,3-dihydro-1H-inden-2-ylamino)ethyl]-3-(trifluoro-

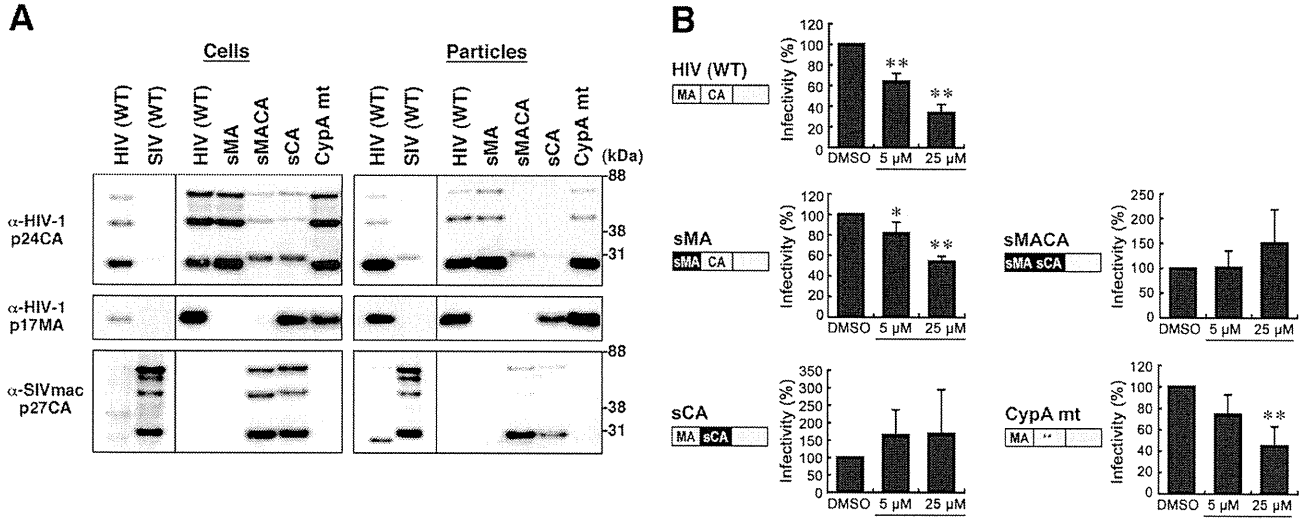

FIG. 6. Mapping of Gag domain responsible for inhibition. (A) Intracellular Gag expression and particle production. 293FT cells were cotransfected with pHIVgag-pol expressing chimeric Gag, pLenti-luciferase, pRevpac, and a plasmid expressing VSV-G, and virus particles produced were purified by ultracentrifugation. Cells and particles were analyzed by Western blotting using anti-HIV-1 p24CA and p17MA and anti-SIVmac p27CA antibodies. (B) Single-round infection assays with the Gag domain chimeras and Gag mutants with amino acid substitutions. The corresponding domain of SIVmac Gag (black) was introduced into HIV-1 Gag background (gray), and the resultant chimera was referred to as "s" plus the name of the corresponding domain of SIVmac. WT, wild type; sMA, HIV containing replacement of MA with SIV MA; sMACA, HIV containing replacement of MACA with SIV MACA; sCA, HIV containing replacement of CA with SIV CA. CypA mt represents HIV with amino acid substitutions G89A and P90A in the CypA-binding loop of CA NTD (denoted by asterisks). Following infection, the cell culture was incubated in the presence of 5 and 25 μM BMMP. Viral infectivity was monitored by luciferase reporter assays. Data were shown as means with standard deviations from 4 to 6 independent experiments. *, $P < 0.05$; **, $P < 0.01$.

methyl)pyridin-2(1H)-one (molecular weight, 454) (7). The hallmark of these inhibitors is incomplete Gag processing and accumulation of processing intermediates (e.g., CA-SP1) in virions, resulting in the loss of viral infectivity. These compounds do not inhibit Gag assembly. Since our BMMP did not show alteration in overall patterns of Gag processing (Fig. 4A), it is unlikely that BMMP shares the inhibition mechanisms with above inhibitors.

Inhibitors of HIV capsid assembly have been extensively screened by several approaches. *In silico* screening from public chemical libraries has identified *N*-(3-chloro-4-methylphenyl)-*N*′-{2-[({5-[(dimethylamino)-methyl]-2-furyl}-methyl)-sulfanyl] ethyl}-urea, termed CAP-1 (32), which binds to HIV-1 CA NTD (K_d [dissociation constant] = 800 μM), resulting in the inhibition of the correct interaction of hexameric units of CA NTD with dimeric units of CA CTD, essential for a high order of CA assembly (20). CAP-1 reduced the infectivity of progeny HIV but did not inhibit viral entry or particle production (32). Phage display biopanning has also been employed and has isolated a 12-mer peptide, termed CAI, which binds to HIV-1 CA CTD (50% inhibitory concentration [IC_{50}] = 3 to 4 μM) and inhibits CA capsid formation *in vitro* (K_d = 15 μM) (5, 29, 33). However, CAI did not inhibit HIV replication in cell culture because of the lack of cell permeability. In a subsequent study, CAI has been converted to a cell-penetrating peptide (termed NYAD-1) by stabilizing the α-helical structure of CAI with a hydrocarbon staple, leading to a marked improvement of K_d (<1 μM) (38). Surprisingly, the study revealed that, besides inhibiting the particle production, NYAD-1 disrupted the mature core formation and inhibited the early stage of HIV-1 in single-round infection assays, suggesting that NYAD-1 may affect the uncoating stage of the HIV life cycle through a mechanism similar to that of BMMP.

The difference between BMMP and CAI/NYAD-1 is that BMMP does not affect HIV-1 particle production or maturation steps. This is possibly because BMMP inhibits CA-CA interactions more efficiently than Gag-Gag interactions. Importantly, BMMP is not a peptide but a low-molecular-weight compound (molecular weight, 273.38), which is chemically and physically stable. It should be possible to chemically modify the BMMP structure to potentiate its biochemical and biological activities. The advantage of BMMP is that, due to its low molecular weight, the derivatives could retain cell membrane permeability unless large chemical groups are attached to the core structure.

A low-molecular-weight Gag inhibitor, PF74, previously screened from a chemical library by a high-throughput single-round infection assay (6), has been characterized by a more recent study, in which PF74 selectively inhibited HIV-1 (27). PF74 destabilized HIV-1 capsids and inhibited the postentry events, similarly to BMMP, but at low-micromolar concentrations. However, BMMP is distinct from PF74 in that the CypA-binding loop is not involved in the viral susceptibility to BMMP (Fig. 6B). Also, BMMP did not reduce the viral infectivity when the virion was exposed to BMMP (data not shown). Therefore, BMMP may have a potential to serve as a lead compound for the development of anti-HIV drugs bearing a novel mechanism of action.

Although BMMP showed anti-HIV activity, it still needs to be improved to lower the IC_{50}. We suggest that comprehensive studies on structural analogues of BMMP would be informative to understand the structure-function relationship of

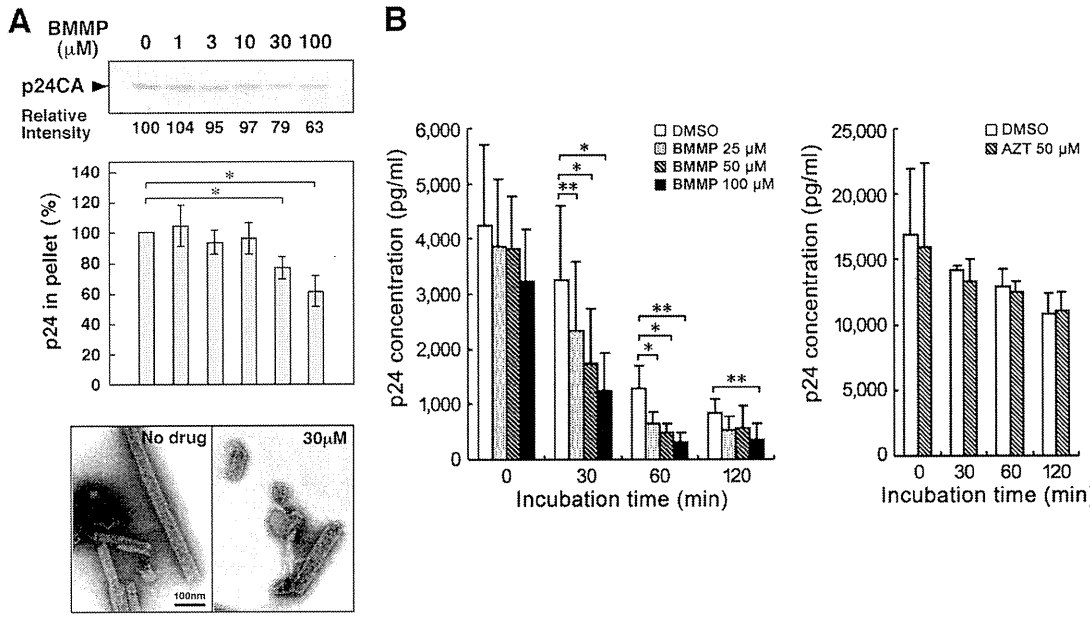

FIG. 7. HIV-1 mature capsid disassembly and *in vitro* assembly assays. (A) *In vitro* assembly reaction with purified HIV-1 CA. Purified HIV-1 CA protein (100 μM) was incubated with various doses of BMMP at 37°C for 60 min in buffer at high salt concentration. All samples included 1% DMSO. Assembly products were recovered by centrifugation and subjected to SDS-PAGE followed by Coomassie brilliant blue staining. The band intensities were semiquantified by ImageJ software. For quantification, the pelleted products were subjected to p24CA antigen capture ELISA. Data were shown as means with standard deviations from 3 independent experiments. *, $P < 0.05$. Assembly products were also negatively stained and examined by electron microscopy. Micrographs were shown at the same magnification. Bar = 100 nm. (B) Cell-free assays for HIV-1 uncoating. HIV-1 mature capsids were isolated through a 1% Triton X-100 layer as described previously (3). The HIV-1 cores were incubated with various doses of BMMP at 37°C up to 120 min. For comparison, the cores were similarly incubated with 50 μM AZT. All samples included 1% DMSO. Residual intact cores were recovered by ultracentrifugation and quantified by p24CA antigen capture ELISA. Data were shown as means with standard deviations from 4 independent experiments. *, $P < 0.05$; **, $P < 0.01$.

BMMP. Also, analysis of BMMP-resistant viruses and X-ray cocrystallography should provide insights into the mechanism of action that direct the way to potentiate the BMMP derivatives.

Recent cryo-electron microscopy and X-ray structure analysis have revealed the intermolecular interfaces between NTD and CTD in the three-dimensional hexameric structures of full-length CA (18, 24). It has been strongly suggested that multiple CA interactions, including NTD-NTD, CTD-CTD, and NTD-CTD, are essential for the constitution of mature HIV capsid. It is possible that some of the interfaces may not be formed in Gag-Gag interactions. CAI, similar to CAP-1, may inhibit CA assembly possibly by disrupting the formation of the NTD-CTD interface (18). Thus, these studies may provide a rationale for developing inhibitors that target the molecular interface of CA that specifically appears during a higher order of oligomerization. We suggest that viral capsid assembly/disassembly is an attractive therapeutic target and that such capsid inhibitors would help understand the regulation of postentry events.

ACKNOWLEDGMENTS

This work was supported by a Human Science grant from the Ministry of Health, Labor, and Welfare of Japan and by a Grant-in-Aid for Scientific Research from the Japan Society for the Promotion of Science.

REFERENCES

1. **Adamson, C. S., et al.** 2006. In vitro resistance to the human immunodeficiency virus type 1 maturation inhibitor PA-457 (Bevirimat). J. Virol. **80:** 10957–10971.
2. **Adamson, C. S., K. Waki, S. D. Ablan, K. Salzwedel, and E. O. Freed.** 2009. Impact of human immunodeficiency virus type 1 resistance to protease inhibitors on evolution of resistance to the maturation inhibitor bevirimat (PA-457). J. Virol. **83:**4884–4894.
3. **Aiken, C.** 2009. Cell-free assays for HIV-1 uncoating. Methods Mol. Biol. **485:**41–53.
4. **Aronheim, A., et al.** 1994. Membrane targeting of the nucleotide exchange factor Sos is sufficient for activating the Ras signaling pathway. Cell **78:**949–961.
5. **Bartonova, V., et al.** 2008. Residues in the HIV-1 capsid assembly inhibitor binding site are essential for maintaining the assembly-competent quaternary structure of the capsid protein. J. Biol. Chem. **283:**32024–32033.
6. **Blair, W. S., et al.** 2005. A novel HIV-1 antiviral high throughput screening approach for the discovery of HIV-1 inhibitors. Antiviral Res. **65:**107–116.
7. **Blair, W. S., et al.** 2009. New small-molecule inhibitor class targeting human immunodeficiency virus type 1 virion maturation. Antimicrob. Agents Chemother. **53:**5080–5087.
8. **Botstein, D.** 1997. Yeast as a model organism. Science **277:**1259–1260.
9. **Braaten, D., E. K. Franke, and J. Luban.** 1996. Cyclophilin A is required for an early step in the life cycle of human immunodeficiency virus type 1 before the initiation of reverse transcription. J. Virol. **70:**3551–3560.
10. **Broder, S.** 2010. The development of antiretroviral therapy and its impact on the HIV-1/AIDS pandemic. Antiviral Res. **85:**1–18.
11. **Bukovsky, A. A., A. Weimann, M. A. Accola, and H. G. Gottlinger.** 1997. Transfer of the HIV-1 cyclophilin-binding site to simian immunodeficiency virus from *Macaca mulatta* can confer both cyclosporin sensitivity and cyclosporin dependence. Proc. Natl. Acad. Sci. U. S. A. **94:**10943–10948.
12. **Butler, S. L., M. S. T. Hansen, and F. D. Bushman.** 2001. A quantitative assay for HIV DNA integration *in vivo*. Nat. Med. **7:**631–634.
13. **Craven, R. C., and L. J. Parent.** 1996. Dynamic interactions of the Gag polyprotein. Curr. Top. Microbiol. Immunol. **214:**65–94.
14. **Forshey, B. M., U. von Schwedler, W. I. Sundquist, and C. Aiken.** 2002.

Formation of a human immunodeficiency virus type 1 core of optimal stability is crucial for viral replication. J. Virol. **76:**5667–5677.
15. **Franke, E. K., H. E. Yuan, and J. Luban.** 1994. Specific incorporation of cyclophilin A into HIV-1 virions. Nature **372:**359–362.
16. **Gamble, T. R., et al.** 1996. Crystal structure of human cyclophilin A bound to the amino-terminal domain of HIV-1 capsid. Cell **87:**1285–1294.
17. **Ganser, B. K., S. Li, V. Y. Klishko, J. T. Finch, and W. I. Sundquist.** 1999. Assembly and analysis of conical models for the HIV-1 core. Science **283:** 80–83.
18. **Ganser-Pornillos, B. K., A. Cheng, and M. Yeager.** 2007. Structure of full-length HIV-1 CA: a model for the mature capsid lattice. Cell **131:**70–79.
19. **Graf Einsiedel, H., et al.** 2002. Deletion analysis of $p16^{INK4a}$ and $p15^{INK4b}$ in relapsed childhood acute lymphoblastic leukemia. Blood **99:**4629–4631.
20. **Kelly, B. N., et al.** 2007. Structure of the antiviral assembly inhibitor CAP-1 complex with the HIV-1 CA protein. J. Mol. Biol. **373:**355–366.
21. **Li, F., et al.** 2003. PA-457: a potent HIV inhibitor that disrupts core condensation by targeting a late step in Gag processing. Proc. Natl. Acad. Sci. U. S. A. **100:**13555–13560.
22. **Morikawa, Y.** 2003. HIV capsid assembly. Curr. HIV Res. **1:**1–14.
23. **Pauwels, R., et al.** 1990. Potent and selective inhibition of HIV-1 replication in vitro by a novel series of TIBO derivatives. Nature **343:**470–474.
24. **Pornillos, O., et al.** 2009. X-ray structures of the hexameric building block of the HIV capsid. Cell **137:**1282–1292.
25. **Roberts, N. A., et al.** 1990. Rational design of peptide-based HIV proteinase inhibitors. Science **248:**358–361.
26. **Sakuragi, S., T. Goto, K. Sano, and Y. Morikawa.** 2002. HIV type 1 Gag virus-like particle budding from spheroplasts of *Saccharomyces cerevisiae*. Proc. Natl. Acad. Sci. U. S. A. **99:**7956–7961.
27. **Shi, J., J. Zhou, V. B. Shah, C. Aiken, and K. Whitby.** 2011. Small molecule inhibition of human immunodeficiency virus type 1 infection by virus capsid destabilization. J. Virol. **85:**542–549.
28. **Shimizu, S., et al.** 2007. Inhibiting lentiviral replication by HEXIM1, a cellular negative regulator of the CDK9/cyclin T complex. AIDS **21:**575–582.
29. **Sticht, J., et al.** 2005. A peptide inhibitor of HIV-1 assembly *in vitro*. Nat. Struct. Mol. Biol. **12:**671–677.
30. **Stremlau, M., et al.** 2006. Specific recognition and accelerated uncoating of retroviral capsids by the TRIM5alpha restriction factor. Proc. Natl. Acad. Sci. U. S. A. **103:**5514–5519.
31. **Suzuki, S., et al.** 2010. Peptide HIV-1 integrase inhibitors from HIV-1 gene products. J. Med. Chem. **53:**5356–5360.
32. **Tang, C., et al.** 2003. Antiviral inhibition of the HIV-1 capsid protein. J. Mol. Biol. **327:**1013–1020.
33. **Ternois, F., J. Sticht, S. Duquerroy, H. G. Krausslich, and F. A. Rey.** 2005. The HIV-1 capsid protein C-terminal domain in complex with a virus assembly inhibitor. Nat. Struct. Mol. Biol. **12:**678–682.
34. **Towers, G. J., et al.** 2003. Cyclophilin A modulates the sensitivity of HIV-1 to host restriction factors. Nat. Med. **9:**1138–1143.
35. **Urano, E., et al.** 2008. Substitution of the myristoylation signal of human immunodeficiency virus type 1 Pr55Gag with the phospholipase C-delta1 pleckstrin homology domain results in infectious pseudovirion production. J. Gen. Virol. **89:**3144–3149.
36. **von Schwedler, U. K., et al.** 1998. Proteolytic refolding of the HIV-1 capsid protein amino-terminus facilitates viral core assembly. EMBO J. **17:**1555–1568.
37. **Westby, M., G. R. Nakayama, S. L. Butler, and W. S. Blair.** 2005. Cell-based and biochemical screening approaches for the discovery of novel HIV-1 inhibitors. Antiviral Res. **67:**121–140.
38. **Zhang, H., et al.** 2008. A cell-penetrating helical peptide as a potential HIV-1 inhibitor. J. Mol. Biol. **378:**565–580.

Gene Therapy (2011) 18, 936–941

www.nature.com/gt

SHORT COMMUNICATION

Protein transduction by pseudotyped lentivirus-like nanoparticles

T Aoki[1,2], K Miyauchi[1,2], E Urano[1], R Ichikawa[1] and J Komano[1]

A simple, efficient and reproducible method to transduce proteins into mammalian cells has not been established. Here we describe a novel protein transduction method based on a lentiviral vector. We have developed a method to package several thousand foreign protein molecules into a lentivirus-like nanoparticle (LENA) and deliver them into mammalian cells. In this proof-of-concept study, we used β-lactamase (BlaM) as a reporter molecule. The amino-terminus of BlaM was fused to the myristoylation signal of *lyn*, which was placed upstream of the amino-terminus of *Gag* (BlaM-gag-pol). By co-transfection of plasmids encoding BlaM-gag-pol and vesicular stomatitis virus-G (VSV-G) into 293T cells, LENA were produced containing BlaM enzyme molecules as many as Gag per capsid, which has been reported to be ~5000 molecules, but lacking the viral genome. Infection of 293T and MT-4 cells by VSV-G-pseudotyped BlaM-containing LENA led to successful transduction of BlaM molecules into the cell cytoplasm, as detected by cleavage of the fluorescent BlaM substrate CCF2-AM. LENA-mediated transient protein transduction does not damage cellular DNA, and the preparation of highly purified protein is not necessary. This technology is potentially useful in various basic and clinical applications.
Gene Therapy (2011) **18,** 936–941; doi:10.1038/gt.2011.38; published online 31 March 2011

Keywords: LENA; BlaM; Gag; protein transduction; lentiviral vector

INTRODUCTION

When viruses infect cells the viral contents are released. A virus can, therefore, be considered as a protein transduction vehicle into a target cell if a large number of foreign proteins are packaged per virion. A lentiviral vector, approved for human gene therapy,[1] has been produced by transfecting 293T cells with four plasmids: the gene transfer vector that provides the viral genome packaged into the virion, and three plasmid vectors, each expressing *gag–pol*, *rev* or the vesicular stomatitis virus-G (VSV-G) genome.[2–4] The *gag–pol* expression vector produces Gag and Gag-pol in a ratio of ~20:1 because of the frameshift signal positioned between the *gag* and *pol* open reading frames.[5] Gag ($Pr55^{Gag}$) is a viral structural protein that traffics to the plasma membrane aided by its amino-terminal myristoyl group, and self-oligomerizes at the plasma membrane to form a spherical structure.[6] The expression of Gag alone leads to the production of an enveloped virus-like particle (VLP) of ~100 nm in diameter, consisting of ~5000 Gag molecules.[7]

When the *gag–pol* expression vector is used to produce VLP, both Gag and Gag-pol proteins, a total of 5000 molecules,[7] form the lentiviral nanoparticles in which approximately one-twentieth of the VLP-forming protein is Gag-pol.[5] The VLP produced by the *gag–pol* expression vector undergoes maturation whereby Gag is processed by the protease made from Pol. Gag is cleaved into $p17^{MA}$, $p24^{CA}$ and other smaller fragments. This changes the shape of the VLP core from doughnut shape to bullet shape, as visualized by electron microscopy. Mediated by VSV-G, the mature VLP envelope fuses to the cell membrane more efficiently than the immature VLP.[8] In accordance with this process, if a foreign protein is fused to lentiviral Gag, a large number of foreign proteins should be transduced into mammalian cells. In this work, the lentiviral vector has been engineered to achieve this goal.

By co-transfecting two plasmid vectors, each expressing *gag–pol* or VSV-G, the lentivirus-like nanoparticles (LENA) can be produced with a VSV-G envelope (Figure 1a). These particles undergo maturation, and should be highly competent for promoting fusion of LENA envelope to the cell membrane. The VSV-G-pseudotyped LENA should be capable of releasing viral content into the target cells. We have named this process 'pseudoinfection' because it mimics viral infection, but is not accompanied by integration of the viral genome into chromosomal DNA.

We have previously shown that substitution of the human immunodeficiency virus type 1 (HIV-1) Gag myristoylation signal with the phospholipase C-δ 1 pleckstrin homology (PH) domain, or attachment of heterologous myristoylation signals to the amino-terminus of Gag, increases the production of lentiviral vector.[9,10] In these studies we used the human codon-optimized *gag–pol* to maximize viral protein synthesis. The infectivity of these pseudovirions was comparable with that of the wild-type (WT) counterpart. This is noteworthy because modification of Gag often results in reduction of viral productivity and infectivity.[11,12] It has been reported recently that a protein transduction using murine leukemia virus is achievable by embedding a foreign gene in *gag*. However, the viral productivity and infectivity need to be improved by WT Gag-pol provided in *trans* upon viral production. These data suggest that by fusing a foreign protein to the amino-terminus of Gag and providing a membrane-targeting signal, it is possible to produce a high-titer, uniform, foreign protein-containing LENA without the need to co-transfect the WT Gag-pol expression plasmid. We tested whether the VSV-G-pseudotyped

[1]AIDS Research Center, National Institute of Infectious Diseases, Shinjuku-ku, Tokyo, Japan
Correspondence: Dr J Komano, AIDS Research Center, National Institute of Infectious Diseases, Toyama, 1-23-1, Shinjuku-ku, Tokyo 162-8640, Japan.
E-mail: ajkomano@nih.go.jp
[2]These authors contributed equally to this work.
Received 29 August 2010; revised 2 December 2010; accepted 3 January 2011; published online 31 March 2011

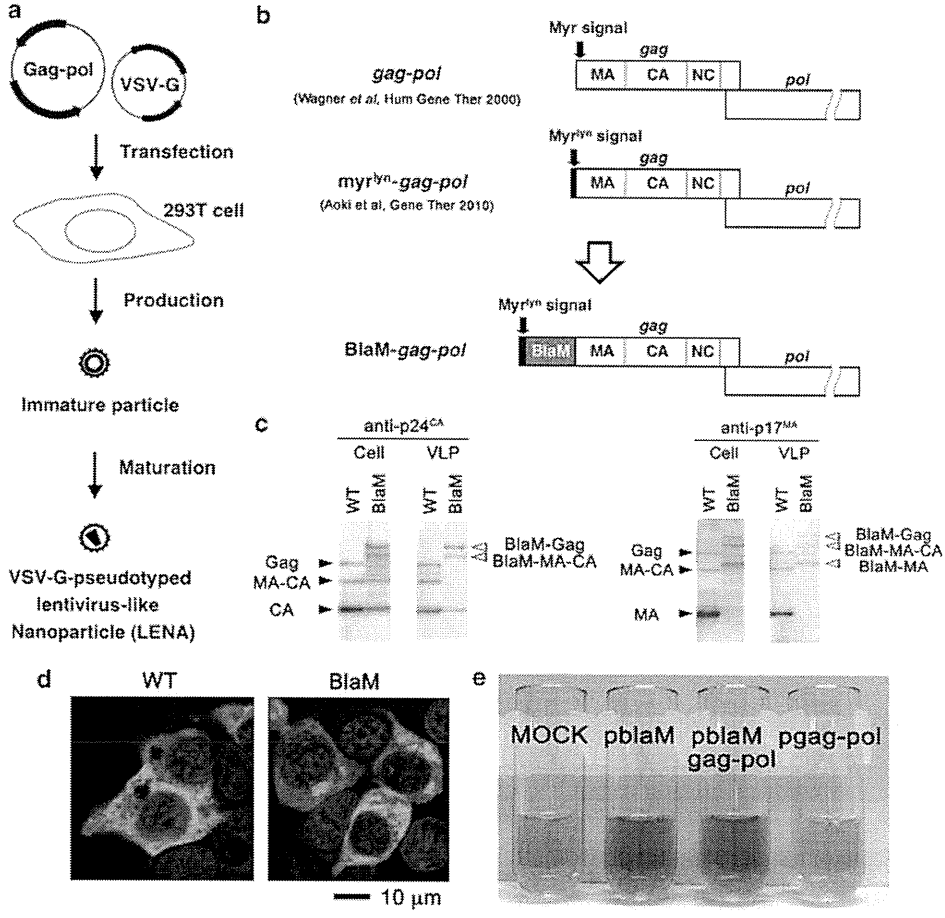

Figure 1 Production of a BlaM-containing LENA pseudotyped with VSV-G. (**a**) Schematic representation of production of VSV-G-pseudotyped LENA. Two plasmids are transfected into 293T cells, and LENA is recovered from the culture supernatant at 48 h post-transfection. The viral protease is activated after the VLP is released from the cell, and it mediates the maturation of the particles. (**b**) The structure of WT *gag–pol*, a mutant bearing the myristoylation signal of *lyn* (myr^{lyn}-*gag-pol*), and *blaM-gag-pol*. Gag is cleaved into p17^{MA} (MA), p24^{CA} (CA), nucleocapsid (NC) and other domains by the viral protease encoded in *pol*. In the myr^{lyn}-*gag-pol* and *blaM-gag-pol* constructs, the Gag translational initiation site and the myristoylation target residues were mutated to leucine and alanine to minimize internal translational initiation and myristoylation. (**c**) Verification of protein expression and VLP production of BlaM-gag-pol construct in 293T cells by western blot analysis using anti-p24^{CA} and anti-p17^{MA} antibodies. Shown are the analyses of cell lysates (Cell) transfected with p*gag-pol* (WT) or p*blaM-gag-pol* (BlaM), and the viral particles (VLP) collected from the culture supernatant of transfected cells. Pr55^{Gag} (~55 kDa, Gag), the Gag proteolytic cleavage intermediate MA–CA (~40 kDa) and the complete proteolytic cleavage product p24^{CA} (~24 kDa, CA) and p17^{MA} (~17 kDa, MA) are indicated by arrowheads. BlaM-Gag, BlaM-MA-CA and BlaM-MA have higher molecular weights because of the attachment of BlaM (~30 kDa) to the MA domain. (**d**) Immunofluorescence assay showing the distribution of WT Gag (WT) or BlaM-Gag (BlaM) in 293T cells transfected with p*gag-pol* or p*blaM-gag-pol*. Green and blue represent the anti-p24^{CA} monoclonal antibody-stained signal and the Hoechst 33258-stained nucleus, respectively. Magnification ×400; scale bar, 10 μm. (**e**) BlaM enzyme activity was tested by nitrocefin. Lysates from 293T cells transfected with p*blaM*, p*blaM-gag-pol*, *or* p*gag-pol* or untransfected cells (MOCK) were incubated with nitrocefin for 30 min at 37 °C.

LENA could serve as a protein transduction vehicle for mammalian cells using β-lactamase (BlaM) as a reporter.

RESULTS AND DISCUSSION

BlaM was chosen as reporter molecule because mammalian cells do not have BlaM activity. Also, a cell-membrane-permeable BlaM substrate is available, which can distinguish LENA content release from cellular endocytosis of LENA that can occur without membrane fusion.[13] *BlaM* was fused to the amino-terminus of *gag–pol*, and the *lyn* myristoylation signal was attached to the amino-terminus of *BlaM* (*BlaM-gag-pol*; Figure 1b). The codon usage of *gag–pol* has been human codon optimized, but bearing the natural −1 frameshift signal at the *gag–pol* junction.[14] Thus, the vector provides the natural Gag to Gag-pol ratio. The BlaM-gag-pol protein was produced in 293T cells as expected (Figure 1c). The *BlaM* construct produced VLP from the transfected cells, although the efficiency was less than with WT *gag–pol* (Figure 1c). The processing efficacy of Gag in BlaM VLP was less efficient compared with the WT as highlighted by the absence of free matrix domain (MA) signal in BlaM VLP, which was because of the lack of HIV-1 protease recognition motif between BlaM and MA (right panel, Figure 1c). In 293T cells transiently transfected with this plasmid, the BlaM-gag-pol fusion protein distribution was similar to that of the WT, although with some aggregation in the cytoplasm (Figure 1d). The BlaM-gag-pol fusion protein retained enzyme activity as demonstrated by its reaction with the BlaM substrate nitrocefin, which changed from a straw color to brown when incubated with

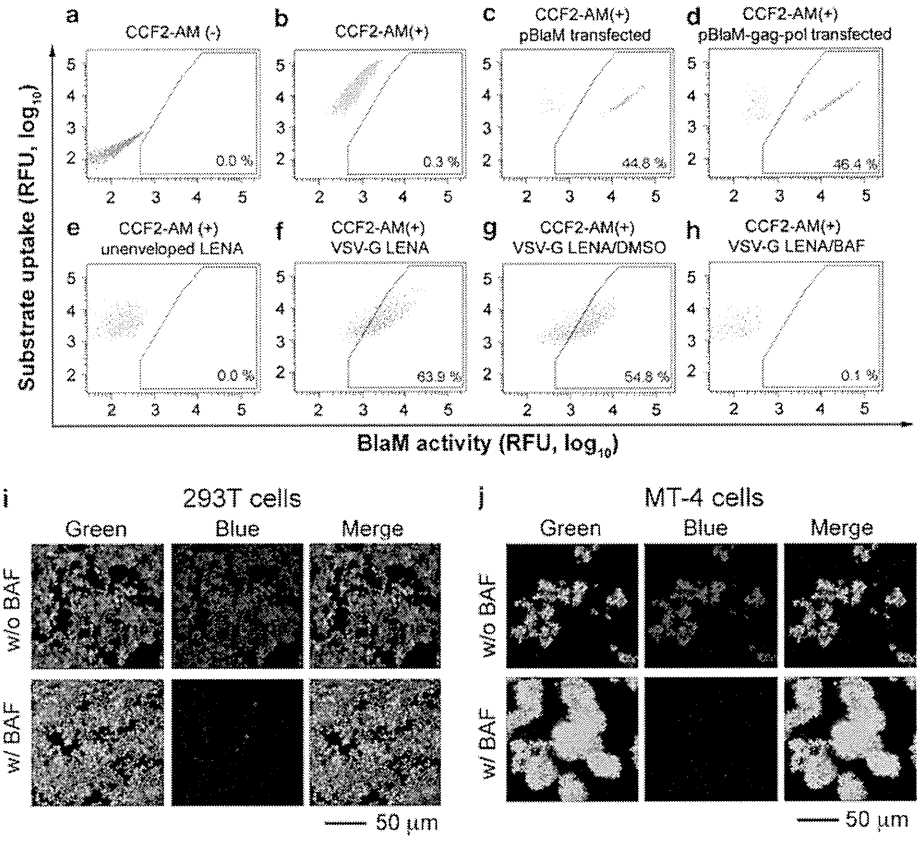

Figure 2 Flow cytometric analysis to measure the BlaM transduction into 293T cells by VSV-G-pseudotyped BlaM-LENA. The 293T cells were grown in 24-well plates and either transfected or pseudoinfected with LENA preparations. (**a**) Unstained 293T cells. (**b**) 293T cells loaded with CCF2-AM. (**c**, **d**) 293T cells were transfected with pBlaM (**c**) or pBlaM-gag-pol (**d**), and loaded with CCF2-AM at 48 h post-transfection before the flow cytometric analysis. (**e–h**) 293T cells were exposed to unenveloped BlaM-LENA (**e**) or VSV-G-pseudotyped BlaM-LENA (**f–h**). Cells were loaded with CCF2-AM at 2 h post-LENA exposure. (**g**, **h**) The VSV-G-dependent BlaM transduction was verified by exposing 293T cells with VSV-G-pseudotyped BlaM-LENA in the presence of bafilomycin A1 (BAF) at a concentration of 10 μg ml^{-1} (**h**). Dimethylsulfoxide (DMSO) was used as a control (**g**). The percentage of the gated population is noted in each panel. The *x* axis represents the blue fluorescence, reflecting the BlaM activity (relative fluorescent unit (RFU)). The *y* axis represents the green fluorescence, reflecting the substrate loading onto the cells. (**i**, **j**) Microscopic detection of BlaM transduction in 293T cells (**i**) or MT-4 cells (**j**) by VSV-G-pseudotyped BlaM-LENA. Cells were exposed to BlaM-LENA for 3 h, and loaded with CCF2-AM overnight at room temperature in the presence (10 μg ml^{-1}) or absence of BAF (w/BAF or w/o BAF, respectively). The bar represents 50 μm, magnification ×200.

lysates from 293T cells transfected with the BlaM-gag-pol expression vector (Figure 1e). The BlaM enzyme activity of BlaM-gag-pol was indistinguishable from that of WT BlaM (Figure 1e). BlaM enzyme activity was not detected in MOCK or p*gag-pol*-transfected cell lysates (Figure 1e).

Protein transduction into 293T cells was conducted by exposing target cells to VSV-G-pseudotyped BlaM-LENA, which mimics viral infection. The success of BlaM transduction into the target cell cytoplasm was judged by using the cytoplasm-retained BlaM substrate, CCF2-AM, which yields blue fluorescence upon cleavage by BlaM enzyme activity.

The 293T cells emitted green fluorescence when they were loaded with CCF2-AM (Figure 2, compare a vs b). When 293T cells were transfected with expression vectors for BlaM or the BlaM-gag-pol, substrate cleavage, as demonstrated by a shift to blue fluorescence, was detected in a discrete population of cells, representing a transfection efficiency of ~45% (Figures 2c and d). These data suggest that transduced BlaM-gag-pol has BlaM activity, consistent with the results of the nitrocefin assay (Figure 1e). When BlaM was transduced into 293T cells by VSV-G-pseudotyped BlaM-LENA, a significant shift from green to blue fluorescence was detected (63.9%, Figure 2f). The rightward shift of the signal along the *x* axis suggests that almost all the cells were transduced with BlaM by BlaM-LENA. BlaM transduction was dependent on VSV-G function as CCF2-AM cleavage was not detected by LENA lacking VSV-G (Figure 2e), and BlaM transduction was inhibited by bafilomycin A1 that blocks VSV-G-mediated membrane fusion (Figure 2, compare g vs h). The catalytic activity was visualized under the fluorescent microscopy. In agreement with the flow cytometric analysis, almost all the substrate-loaded 293T cells exposed to BlaM-LENA became blue fluorescent in experimental conditions comparable with the above experiments, and the catalytic activity was not detected when cells were treated with bafilomycin A1 (Figure 2i). The blue fluorescence was detected homogenously in the cell cytoplasm (Figure 2i). These data were reproduced in human T-cell line MT-4 (Figure 2j). Considering the critical dependence to VSV-G, it is highly unlikely that the BlaM activity was derived from the residual DNA/lipid mixture in the LENA preparation. The BlaM-transducing unit into 293T cells was $\sim 0.8 \pm 0.01 \times 10^9$ ml^{-1} as

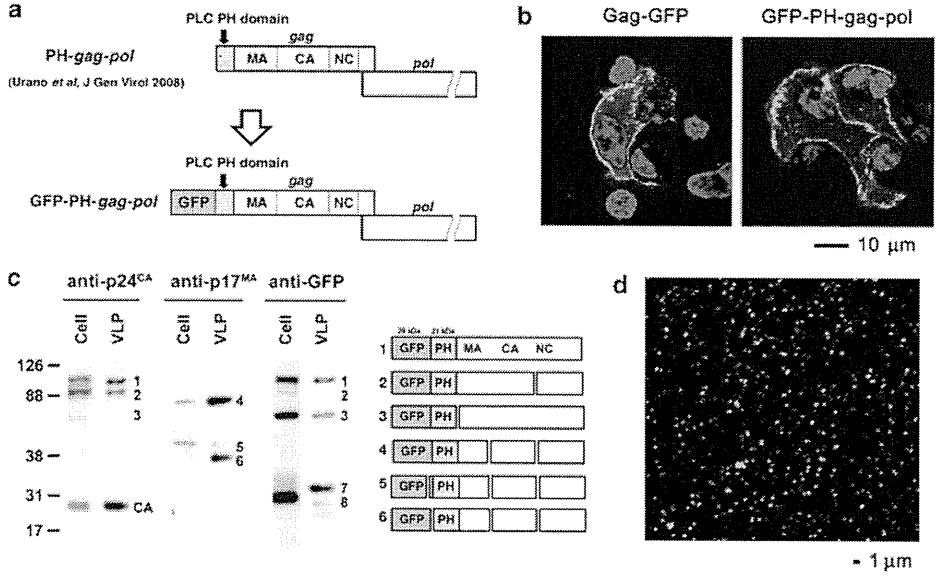

Figure 3 Production of a GFP-containing lentivirus-like nanoparticle for physical counting. (**a**) The structure of PH-*gag-pol* and GFP-PH-*gag-pol*. (**b**) The distribution of Gag-GFP and GFP-PH-gag-pol in transiently transfected 293T cells examined by confocal microscopy. The images were taken at 24 h post-transfection. The bar represents 10 μm, magnification ×630. (**c**) Verification of protein expression and VLP production of GFP-PH-gag-pol construct in 293T cells by western blot analysis using anti-$p24^{CA}$, anti-$p17^{MA}$ and anti-GFP antibodies. Shown are the analyses of cell lysates (Cell) transfected with pGFP-PH-*gag-pol* and the viral particles (VLP) collected from the culture supernatant of transfected cells. The numbers represent the proteolytic products as illustrated in the right panel estimated from the western blot analysis. (**d**) Confocal image of the GFP-PH-LENA on the slide glass. The bar represents 1 μm, magnification ×630.

estimated by the BlaM-LENA serial dilution (data not shown). Thus, 293T cells were exposed to ~1000-fold excess of BlaM-LENA.

We constructed GFP-PH-LENA to visualize the LENA particles (Figure 3a). In this construct, the PH domain from phospholipase C-δ 1 functions as the membrane targeting motif.[9,10] The GFP-PH-gag-pol was distributed at cell periphery, similar to Gag-GFP (Figure 3b). The VLP production by GFP-PH-gag-pol was verified in western blot analysis (Figure 3c). According to the estimated molecular weight of protease-mediated cleavage products, we speculate the possible protease recognition sites within green fluorescent protein (GFP), GFP–PH junction and PH–MA junction, although we did not intentionally reconstitute the HIV-1 protease recognition sites in these positions (Figure 3c). The GFP-encapsidated LENA preparations were spotted onto the poly-L-lysine-coated slide glass, and the captured LENA was imaged by the confocal microscopy. By counting the green fluorescent dot signals per unit area, we estimated the number of GFP-PH-LENA particles as $1.4 \pm 0.2 \times 10^9$ ml^{-1} (Figure 3d), which was similar to the BlaM-transduction unit of VSV-G-pseudotyped BlaM-LENA.

To test whether the lentivirus vector used to produce BlaM-LENA retained any viral infectivity, a lentivirus vector was produced carrying the luciferase gene, using the four plasmid system[9,10] with the BlaM-gag-pol construct, and then viral infectivity was assessed. Gene transduction by this lentiviral vector was undetectable. These data indicate that transfer to target cells by BlaM-LENA of an expressed, endogenous retroviral element from 293T cells is unlikely to occur. These data show that a protein transduction system based on LENA would have an extra level of safety compared with the protein transduction system based on a retroviral vector system.[11]

Protein transduction in a broad sense, referring to the transport of protein across the cell membrane, is a useful technique in experimental molecular biology. It does not require *de novo* transcription and translation, and the transferred protein functions immediately after the transduction. Proteins, however, do not easily pass through the plasma membrane. Historically, microinjection, electroporation and cell-permeable peptide motifs were used to introduce proteins into cells.[15–17] These methods, however, demand a highly purified protein, technical skill or specialized, costly equipment. Also, variable results have been obtained using different proteins and target cells. The need of a highly purified protein applies to protein lipofection to yield the reproducible results. A convenient, fast, highly efficient and reproducible protein transduction method has so far remained undeveloped. Such a technique would greatly help the generation of safe, induced pluripotent stem cells. LENA production is as straightforward as co-transfecting two plasmids into 293T cells without *trans*-complementing the WT *gag–pol* expression vector, and furthermore the therapeutic protein is protected from plasma proteases by a lipid bilayer. The target cell tropism can be controlled by well-established viral pseudotype techniques. Using LENA, a substantial number of protein molecules can be packaged into the nanoparticles, and the transduction procedure is as easy as exposing mammalian cells with LENA. There is no need to prepare highly purified proteins for the LENA system. Also, target proteins are post-translationally modified in human cells, which should be better than the protein modification in non-human organisms. It should also be possible to increase the amount of protein that can be delivered into cells by concentrating the LENA preparation. Physical counting of GFP-encapsidated LENA shows that a high-titer LENA preparation was casually produced. In this study, we did not introduce protease recognition sites into myristoylation signal-BlaM or -BlaM-MA junctions. By doing so, we would have possibly liberated the foreign protein from the precursor. This could result in infectious LENA particles as the free MA is in part important for the viral infectivity.[9]

Currently, few approaches are available for the incorporation of a foreign protein into retro- or lenti-viral VLP. The protein of interest

can be fused to the C-terminus of Gag or inserted into the middle of the Gag protein (for example, between the MA and CA).[11,12] Foreign protein fusion to the C-terminus of Gag would destroy the frameshift signal required to produce Gag-pol. Thus, Pol would no longer be produced. To maintain efficient pseudoinfection, the *gag–pol* expression vector must be provided in *trans* when the VLP is produced. The latter approach often results in reduced VLP yield. Thus, again, to increase the VLP yield, the *gag–pol* expression vector has to be co-transfected with the plasmid encoding Gag fused to the foreign protein. Co-transfection of the *gag–pol* expression vector is likely to reduce the amount of foreign protein per VLP, and lower its uniformity. It is, therefore, desirable not to co-transfect with the WT *gag–pol* expression plasmid. Alternatively, Vpr can be used to incorporate foreign proteins into lentiviral particles.[18] Only a few dozen protein molecules, however, are packed per particle, rendering this approach of little use in protein transduction. In summary, fusion of a foreign protein to the N-terminus of Gag has the advantages of producing uniform, high-titer and membrane fusion-competent VLP without *trans*-complementation by WT Gag-pol.

The disadvantages of the LENA system are the susceptibility of foreign proteins to viral protease and the restriction in the molecular sizes of foreign proteins. We have succeeded in generating Gag-LacZ VLP, suggesting that the production of LENA carrying a foreign protein with a molecular weight of ~100 kDa is feasible. The yield, however, of LENA gradually decreases as the molecular weight of the foreign protein increases. We did not detect proteolytic cleavage of BlaM by viral protease in LENA particles; however, when we tested the transcriptional regulator of HTLV-1 (human T-cell leukemia virus type 1), Tax, it was degraded by viral protease. To overcome these potential disadvantages, it is worth considering the use of only the minimal functional domain of a foreign protein and the destruction of potential protease recognition sites in the foreign protein without losing its function.

Lentiviral vectors have been approved for human gene therapy.[1] LENA does not contain a viral genome, and is unlikely to support the transfer of endogenous retrovirus-like elements; thus, the cellular genome is not threatened by LENA-mediated protein transduction. Thus, a major safety concern associated with retroviral or lentiviral vectors is alleviated, making LENA applicable for *in vivo* studies. Retroviral vectors are often used for induced pluripotent stem cell genesis.[19] However, they can damage the cellular genome, and transduced gene expression is difficult to shut off, which can lead to malignant transformation of induced pluripotent stem cells. To overcome this problem, a transient and efficient protein transduction method is needed. We believe that LENA addresses these issues. Altogether, our system has many advantages over currently available protein transduction protocols, suggesting that it should be considered for basic and clinical applications.

MATERIALS AND METHODS

Plasmids

The following oligonucleotides were annealed, and cloned into the *AfeI–AgeI* sites of pEGFP-C2 (Clontech, Palo Alto, CA, USA) to generate the p*lyn*MyEGFP-C2: 5′-GCTACCGGACTCAGATCTCGAGCTCAAGCTTCGAATTGC CACCATGGGATGTATTAAATCAAAAAGGAAAGACGATCCA-3′ and 5′-CCG GTGGATCGTCTTTCCTTTTTGATTTAATACATCCCATGGTGGCAATTCGA AGCTTGAGCTCGAGATCTGAGTCCGGTAGC-3′. The *SnaBI–EcoRI* fragment from p*lyn*MyEGFP-C2 was cloned into the corresponding sites of pPH-*gag-pol*,[9] generating p*lyn*MyGFP-*gag-pol*. The β-lactamase gene from pUC19 was amplified by the following primers: 5′-ACCGGTCAATCCAGAAACGCTGGTG AAAG-3′ and 5′-CAATTGCCAATGCTTAATCAGTGAGGC-3′. The *AgeI–MfeI* fragment of the PCR fragment was cloned into the *AgeI–EcoRI* sites of p*lyn*MyGFP-*gag-pol*, generating the p*blaM-gag-pol*. The expression vector for VSV-G was described previously.[20] The original codon-optimized HIV-1 *gag–pol* expression vector was described previously.[14] The Gag-GFP expression vector was described previously.[10] The pGFP-PH-*gag-pol* was constructed by inserting the *NdeI–PshAI* fragment from pEGFP-PLCd1 PH[21] into the corresponding sites of pPH-*gag-pol*.[9] pcDNA3 was obtained from Invitrogen (Tokyo, Japan).

Cells and transfection

The 293T cells, obtained from Invitrogen as 293FT cells (Invitrogen), were maintained in RPMI-1640 medium (Sigma, St Louis, MA, USA) supplemented with 10% fetal bovine serum (Japan Bioserum, Tokyo, Japan), 50 U ml^{-1} penicillin and 50 μg ml^{-1} streptomycin (Invitrogen), at 37 °C in a humidified 5% CO_2 atmosphere. Cells were transfected with DNA using Lipofectamine 2000 according to the manufacturer's protocol (Invitrogen), or calcium phosphate precipitation. To produce VSV-G-pseudotyped BlaM-LENA, equal amounts of pVSV-G and p*blaM-gag-pol* were transfected into 293T cells. Unenveloped BlaM-LENA was produced using pcDNA3 in place of pVSV-G.

Immunological detection

The detection of viral gene products by western blot analysis was performed as described previously,[22] except that the anti-p24^{CA} monoclonal antibody clone 183-H12-5C and the anti-p17^{MA} rabbit antiserum (NIH AIDS Research and Reference Reagent Program) were used. The immunofluorescent analysis was performed as described previously,[22] except that cells were fixed at 24 h post-transfection, and the following reagents were used: anti-p24^{CA} monoclonal antibody (clone 183-H12-5C), anti-mouse antibody conjugated with biotin (Invitrogen) and streptavidin conjugated with Alexa488 (Invitrogen).

Microscopy

Cells and GFP-encapsidated LENA were imaged by confocal fluorescence microscopy (LSM510 Meta 40× NA 1.4 lens; Carl Zeiss MicroImaging Inc., Tokyo, Japan).

Colorimetric detection of BlaM activity

Transfected 293T cells grown in 6 cm dishes were lysed in 500 μl of buffer A (10 mM HEPES, 1.5 mM $MgCl_2$, 10 mM KCl and 0.05% IGEPAL CA-630), and then 1 μl of nitrocefin (10 μg ml^{-1}; Calbiochem, San Diego, CA, USA) was added to the cell lysate. The mixture was incubated for 20 min at 37 °C.

Protein transduction

The pseudoinfection was performed as infecting cells with retroviral vectors[20] by incubating ~1×10^6 cells with 1 ml LENA-containing culture medium at 37 °C for 1–3 h in the presence of dextran (final concentration 16.25 μg ml^{-1}; DEAE-Dextran chloride, molecular weight ~500 kDa; ICN Biomedicals Inc., Aurora, OH, USA). The cells were assayed by flow cytometry or fluorescent microscopy after the LENA exposure. Bafilomycin A1 was purchased from Sigma.

Fluorescent detection of BlaM activity

A fluorescence-activated cell sorter Aria (Becton Dickinson, San Jose, CA, USA) was used to detect the CCF2-AM (Invitrogen) signals from 293T cells. A violet 407 nm laser was used for fluorescence activation, and BP450/40 nm and LP502 in conjunction with BP530/30 filters were used for the fluorescent signal detection of cleaved and uncleaved substrates, respectively. The CCF2-AM signals from 293T and MT-4 cells were imaged by Biorevo (BZ-9000, Keyence, Osaka, Japan) using the blue filter set (excitation, band pass filters 377/50 nm wavelength; emission, band pass 447/60 nm wavelength; dichroic mirror, 409 nm wavelength) and the green filter set (excitation, band pass filters 377/50 nm wavelength; emission, band pass 520/35 nm wavelength; dichroic mirror, 495 nm wavelength).

CONFLICT OF INTEREST

The authors declare no conflict of interest.

ACKNOWLEDGEMENTS

This work was supported by the Japan Health Science Foundation, the Japanese Ministry of Health, Labor, and Welfare (H18-AIDS-W-003 to JK) and the Japanese Ministry of Education, Culture, Sports, Science and Technology (18689014 and 18659136 to JK).

1 MacGregor RR. Clinical protocol. A phase 1 open-label clinical trial of the safety and tolerability of single escalating doses of autologous CD4 T cells transduced with VRX496 in HIV-positive subjects. *Hum Gene Ther* 2001; **12**: 2028–2029.
2 Cockrell AS, Kafri T. Gene delivery by lentivirus vectors. *Mol Biotechnol* 2007; **36**: 184–204.
3 McCart JA, Bartlett DI. Lentiviral Vectors. In: Templeton NS (ed.). *Gene and Cell Therapy: Therapeutic Mechanisms and Strategies*, 3rd edn. CRC Press: Carrollton, 2008, pp 245–262.
4 Lundberg C, Björklund T, Carlsson T, Jakobsson J, Hantraye P, Déglon N *et al.* Applications of lentiviral vectors for biology and gene therapy of neurological disorders. *Curr Gene Ther* 2008; **8**: 461–473.
5 Jacks T, Power MD, Masiarz FR, Luciw PA, Barr PJ, Varmus HE. Characterization of ribosomal frameshifting in HIV-1 gag-pol expression. *Nature* 1988; **331**: 280–283.
6 Klein KC, Reed JC, Lingappa JR. Intracellular destinies: degradation, targeting, assembly, and endocytosis of HIV Gag. *AIDS Rev* 2007; **9**: 150–161.
7 Briggs JA, Simon MN, Gross I, Kräusslich HG, Fuller SD, Vogt VM *et al.* The stoichiometry of Gag protein in HIV-1. *Nat Struct Mol Biol* 2004; **11**: 672–675.
8 Wyma DJ, Jiang J, Shi J, Zhou J, Lineberger JE, Miller MD *et al.* Coupling of human immunodeficiency virus type 1 fusion to virion maturation: a novel role of the gp41 cytoplasmic tail. *J Virol* 2004; **78**: 3429–3435.
9 Urano E, Aoki T, Futahashi Y, Murakami T, Morikawa Y, Yamamoto N *et al.* Substitution of the myristoylation signal of human immunodeficiency virus type 1 Pr55Gag with the phospholipase C-delta1 pleckstrin homology domain results in infectious pseudovirion production. *J Gen Virol* 2008; **89**: 3144–3149.
10 Aoki T, Shimizu S, Urano E, Futahashi Y, Hamatake M, Tamamura H *et al.* Improvement of lentiviral vector-mediated gene transduction by genetic engineering of the structural protein Pr55(Gag). *Gene Therapy* 2010; **17**: 1124–1133.
11 Voelkel C, Galla M, Maetzig T, Warlich E, Kuehle J, Zychlinski D *et al.* Protein transduction from retroviral Gag precursors. *Proc Natl Acad Sci USA* 2010; **107**: 7805–7810.
12 Hubner W, Chen P, Del Portillo A, Liu Y, Gordon RE, Chen BK. Sequence of human immunodeficiency virus type 1 (HIV-1) Gag localization and oligomerization monitored with live confocal imaging of a replication-competent, fluorescently tagged HIV-1. *J Virol* 2007; **81**: 12596–12607.
13 Campbell RE. Realization of beta-lactamase as a versatile fluorogenic reporter. *Trends Biotechnol* 2004; **22**: 208–211.
14 Wagner R, Graf M, Bieler K, Wolf H, Grunwald T, Foley P *et al.* Rev-independent expression of synthetic gag-pol genes of human immunodeficiency virus type 1 and simian immunodeficiency virus: implications for the safety of lentiviral vectors. *Hum Gene Ther* 2000; **11**: 2403–2413.
15 Ulett GA, Han S, Han JS. Electroacupuncture: mechanisms and clinical application. *Biol Psychiatry* 1998; **44**: 129–138.
16 Ford KG, Souberbielle BE, Darling D, Farzaneh F. Protein transduction: an alternative to genetic intervention? *Gene Therapy* 2001; **8**: 1–4.
17 Zhang Y, Yu LC. Microinjection as a tool of mechanical delivery. *Curr Opin Biotechnol* 2008; **19**: 506–510.
18 Cavrois M, De Noronha C, Greene WC. A sensitive and specific enzyme-based assay detecting HIV-1 virion fusion in primary T lymphocytes. *Nat Biotechnol* 2002; **20**: 1151–1154.
19 Yamanaka S, Blau HM. Nuclear reprogramming to a pluripotent state by three approaches. *Nature* 2010; **465**: 704–712.
20 Komano J, Miyauchi K, Matsuda Z, Yamamoto N. Inhibiting the Arp2/3 complex limits infection of both intracellular mature vaccinia virus and primate lentiviruses. *Mol Biol Cell* 2004; **15**: 5197–5207.
21 Stauffer TP, Ahn S, Meyer T. Receptor-induced transient reduction in plasma membrane PtdIns(4,5)P2 concentration monitored in living cells. *Curr Biol* 1998; **8**: 343–346.
22 Miyauchi K, Komano J, Yokomaku Y, Sugiura W, Yamamoto N, Matsuda Z. Role of the specific amino acid sequence of the membrane-spanning domain of human immunodeficiency virus type 1 in membrane fusion. *J Virol* 2005; **79**: 4720–4729.

Two Genetic Determinants Acquired Late in *Mus* Evolution Regulate the Inclusion of Exon 5, which Alters Mouse APOBEC3 Translation Efficiency

Jun Li[1], Yoshiyuki Hakata[1]*, Eri Takeda[1¤], Qingping Liu[2], Yasumasa Iwatani[3], Christine A. Kozak[2], Masaaki Miyazawa[1]*

1 Department of Immunology, Kinki University School of Medicine, Osaka, Japan, **2** Laboratory of Molecular Microbiology, National Institute of Allergy and Infectious Diseases, National Institutes of Health, Bethesda, Maryland, United States of America, **3** Department of Infection and Immunology, Clinical Research Center, Nagoya Medical Center, Nagoya, Japan

Abstract

Mouse apolipoprotein B mRNA-editing enzyme catalytic polypeptide-like editing complex 3 (mA3), an intracellular antiviral factor, has 2 allelic variations that are linked with different susceptibilities to beta- and gammaretrovirus infections among various mouse strains. In virus-resistant C57BL/6 (B6) mice, mA3 transcripts are more abundant than those in susceptible BALB/c mice both in the spleen and bone marrow. These strains of mice also express mA3 transcripts with different splicing patterns: B6 mice preferentially express exon 5-deficient (Δ5) mA3 mRNA, while BALB/c mice produce exon 5-containing full-length mA3 mRNA as the major transcript. Although the protein product of the Δ5 mRNA exerts stronger antiretroviral activities than the full-length protein, how exon 5 affects mA3 antiviral activity, as well as the genetic mechanisms regulating exon 5 inclusion into the mA3 transcripts, remains largely uncharacterized. Here we show that mA3 exon 5 is indeed a functional element that influences protein synthesis at a post-transcriptional level. We further employed *in vitro* splicing assays using genomic DNA clones to identify two critical polymorphisms affecting the inclusion of exon 5 into mA3 transcripts: the number of TCCT repeats upstream of exon 5 and the single nucleotide polymorphism within exon 5 located 12 bases upstream of the exon 5/intron 5 boundary. Distribution of the above polymorphisms among different *Mus* species indicates that the inclusion of exon 5 into mA3 mRNA is a relatively recent event in the evolution of mice. The widespread geographic distribution of this exon 5-including genetic variant suggests that in some *Mus* populations the cost of maintaining an effective but mutagenic enzyme may outweigh its antiviral function.

Citation: Li J, Hakata Y, Takeda E, Liu Q, Iwatani Y, et al. (2012) Two Genetic Determinants Acquired Late in *Mus* Evolution Regulate the Inclusion of Exon 5, which Alters Mouse APOBEC3 Translation Efficiency. PLoS Pathog 8(1): e1002478. doi:10.1371/journal.ppat.1002478

Editor: Sara Sawyer, University of Texas at Austin, United States of America

Received July 5, 2011; **Accepted** November 26, 2011; **Published** January 19, 2012

Funding: This work was supported by grants-in-aid for Scientific Research from the Ministry of Education, Culture, Sports, Science and Technology of Japan, including the High-Tech Research Center and Anti-Aging Center projects, those from the Japan Society for Promotion of Sciences, KAKENHI (B), and those from the Ministry of Health, Labor and Welfare of Japan for Research on HIV/AIDS (all given to MM), and by a Grant-in-Aid for Young Scientists (B) from the Japan Society for the Promotion of Sciences, KAKENHI 21790450, given to YH. This work was also supported by the Intramural Research Program of the NIH, NIAID, given to CAK. The funders had no role in study design, data collection and analysis, decision to publish, or preparation of the manuscript.

Competing Interests: The authors have declared that no competing interests exist.

* E-mail: hakata@med.kindai.ac.jp (YH); masaaki@med.kindai.ac.jp (MM)

¤ Current address: Department of Emerging Infectious Diseases, Nagasaki University Institute of Tropical Medicine, Nagasaki, Japan

Introduction

The family of apolipoprotein B mRNA-editing enzyme catalytic polypeptide-like editing complex 3 (APOBEC3) proteins consists of cytidine deaminases that function as cellular restriction factors against various exogenous and endogenous viruses [1–17]. Seven APOBEC3 paralogues have been identified on human chromosome 22, while only a single copy of the *Apobec3* gene is found in the mouse genome [10,18,19]. Among the human APOBEC3 enzymes, APOBEC3G (hA3G) is the best characterized member and is known to inhibit HIV-1 replication when the virus lacks the functional accessory protein, viral infectivity factor (Vif) [reviewed in 20]. In the absence of Vif, hA3G is incorporated into newly generated virions budding from virus-producing cells and exhibits its antiviral effect in subsequently infected cells. Thus, during reverse transcription in the target cells, the virion-incorporated hA3G catalyzes C-to-U deamination on the minus strand of nascent viral DNA, resulting in G-to-A mutations on the plus strand of the double-stranded viral DNA, which can be detrimental to viral replication [7,9,10,21,22]. In addition, a deaminase-independent antiviral mechanism exerted by hA3G has also been reported [23,24].

In contrast to its human counterparts, mouse APOBEC3 (mA3) restricts HIV-1 regardless of the presence of Vif, as well as mouse mammary tumor virus (MMTV), ecotropic murine leukemia viruses (MuLVs), Friend MuLV (F-MuLV) and Moloney MuLV (M-MuLV), along with endogenous mouse retroviruses including the AKR ecotropic virus (AKV) [5,25–30]. This suggests that APOBEC3 enzymes protect host genomes from the retroviruses they commonly encounter, although some retroviruses, like HIV-1, have evolved to counter the intracellular restriction mechanisms of their natural hosts.

Friend virus (FV) is an acutely leukemogenic retroviral complex composed of replication-competent F-MuLV and replication

Author Summary

Susceptibility to acutely leukemogenic Friend virus (FV) retrovirus infection varies among different mouse strains and is governed by several genetic factors, one of which is allelic variations at the mouse *Apobec3* locus. FV-resistant C57BL/6 (B6) mice express higher amounts of *Apobec3* transcripts than susceptible BALB/c mice. We previously showed that the differences in N-terminal amino acid sequences between B6 and BALB/c APOBEC3 proteins partly account for the distinct antiretroviral activities. In addition, B6 and BALB/c mice express major *Apobec3* transcripts of different sizes: the exon 5-lacking and the full-length transcripts, respectively. Here we asked if exon 5 has any role in the antiviral activity of mouse APOBEC3 and found that the presence of this exon resulted in a profound decrease in the efficiency of protein synthesis without affecting the mRNA expression levels. We also identified two genomic polymorphisms that control the inclusion of exon 5 into the *Apobec3* message: the number of TCCT repeats in intron 4 and a single nucleotide polymorphism within exon 5. The distribution of these functional polymorphisms among *Mus* species and wild mouse populations indicates that the exon 5 inclusion occurred recently in *Mus* evolution, and the full-length variant may have selective advantages in some mouse populations.

-defective spleen focus-forming virus (SFFV). Susceptibilities to FV-induced disease development differ among various inbred strains of mice, and these are controlled by several host factors that either directly affect FV replication or influence host immune responses to the viral antigens [31,32]. We and others have reported that the mouse *Apobec3* locus is polymorphic, and its genotypes are associated with the levels of viremia after F-MuLV or FV inoculation [26,27]. Mice of the prototypic FV-resistant strains C57BL/6 (B6) and C57BL/10 exhibit restricted replication of F-MuLV and earlier production of FV-neutralizing antibodies, while FV-susceptible BALB/c and A strains are less restrictive of F-MuLV replication and show delayed production of neutralizing antibodies, all of which are linked with *Apobec3* genotypes [26,27,33,34], although the production of neutralizing antibodies is also influenced by genotypes at the major histocompatibility complex and the *Tnfrsf13c* loci, the latter of which encode the receptor for B-cell activating factor belonging to the tumor necrosis factor family [31–33,35].

Mouse APOBEC3 and hA3G contain two cytidine deaminase domains (CDDs), each harboring the conserved zinc-coordinating motif; however, deaminase activity is exerted only by the N-terminal CDD of mA3 and the C-terminal CDD of hA3G [36]. We showed that the increased efficiency of B6 mA3 in inhibiting F-MuLV replication is associated with differences in the primary amino acid sequence within the active N-terminal CDD [27]; the functional importance of these residues was further implicated by the demonstration that they have been under positive selection in *Mus* [37]. In addition to the above sequence differences in the protein-coding regions, efficient virus restriction is also associated with higher levels of mA3 transcripts in FV-resistant B6 than in -susceptible BALB/c mice [27,29,38,39]. This enhanced transcription was linked with the presence of the long terminal repeat (LTR) of an endogenized xenotropic MuLV in the B6, but not in the BALB/c, *Apobec3* locus [37]. A third factor associated with virus resistance is the presence or absence of exon 5, which encodes a 33-amino acid segment separating the C-terminal and N-terminal CDDs [27]. The mA3 isoform of the FV-resistant strains of mice lacks exon 5, while the predominant transcript in FV-susceptible mice is the exon 5-containing isoform [27,29,37]. Genetic sequences controlling mA3 splicing have not been identified, although it has been pointed out that polymorphisms between the B6 and BALB/c *Apobec3* alleles at the end of intron 4 include a putative splice acceptor site and possible mRNA branch selection site structures [38]. It has also not been shown whether the well-confirmed differences in transcript levels result in altered expression levels of mA3 protein in FV-resistant and -susceptible strains of mice.

In the present report, we show that mA3 protein is indeed more abundant in B6 than in BALB/c mice. This difference is due in part to more efficient translation of the exon 5-deficient message. We further show extensive functional evidence that two distinct polymorphisms within the *Apobec3* locus regulate exon 5 inclusion during its splicing: the previously predicted [38] TCCT repeat numbers in intron 4 and a newly identified single nucleotide polymorphism (SNP) within exon 5. We also describe the linkage between these splicing regulatory sequences in wild mouse species, their acquisition in *Mus* evolution, and their distribution in wild mouse populations.

Results

APOBEC3 expression is higher in B6 than in BALB/c spleens at both transcriptional and protein levels

It has been reported that mA3 mRNA expression is higher in B6 than in BALB/c mice, and the mA3 transcripts detected in B6 mice are predominantly the exon 5-lacking Δ5 isoform, while the majority of mA3 transcripts in BALB/c mice contain exon 5 (5+) [27,29,38]. To more accurately describe the above quantitative differences in mA3 transcripts, we performed two types of PCR analyses with two different sets of specific primers (Figure 1A). The primer set c–d, which is the same as the one previously used [27], detected both the 5+ and Δ5 transcripts in reverse-transcription PCR (RT-PCR) assays; however, mA3 transcripts were barely detectable after 30 cycles of amplification in BALB/c mice while the Δ5 transcript was readily detectable in B6 mice (Figure 1B). After 35 cycles of amplification, both the 5+ and Δ5 transcripts became detectable in BALB/c mice, although the 5+ mRNA was more abundant. Quantitative real-time PCR (qPCR) assays revealed mA3 expression levels that were approximately 18-times higher in B6 than in BALB/c spleens, although the difference in transcript lengths might have influenced the efficiencies of amplification in the real-time PCR reactions. To more precisely quantify the mA3 transcripts, we utilized the second primer set, a–b, which generates amplicons of the same size from both alleles (Figure 1A). The qPCR assay performed by using this latter primer set clearly demonstrated that B6 mice expressed >7-times higher amounts of mA3 transcript than BALB/c mice did (Figure 1C), consistent with the previous report [27]. The normalization of mA3 mRNA levels with TATA box-binding protein or GAPDH transcripts instead of β-actin gave similar results (data not shown).

Protein levels of mA3 in the above prototypic FV-resistant and -susceptible strains of mice were also compared. The spleen lysate from the mA3-knockout mice [40] was used as a negative control. In B6 spleens, an immunoreactive protein corresponding to Δ5 mA3 was detected as a prominent band, but the higher molecular weight 5+ mA3 was also faintly detectable (Figure 1D), even though the 5+ message was barely detectable by RT-PCR in the present study (Figure 1B) and in the previous reports [27,29]. On the other hand, only the 5+ mA3 protein was detected, with a much lower intensity, in BALB/c spleens. The immunoblotting assays thus demonstrated that the level of total mA3 protein

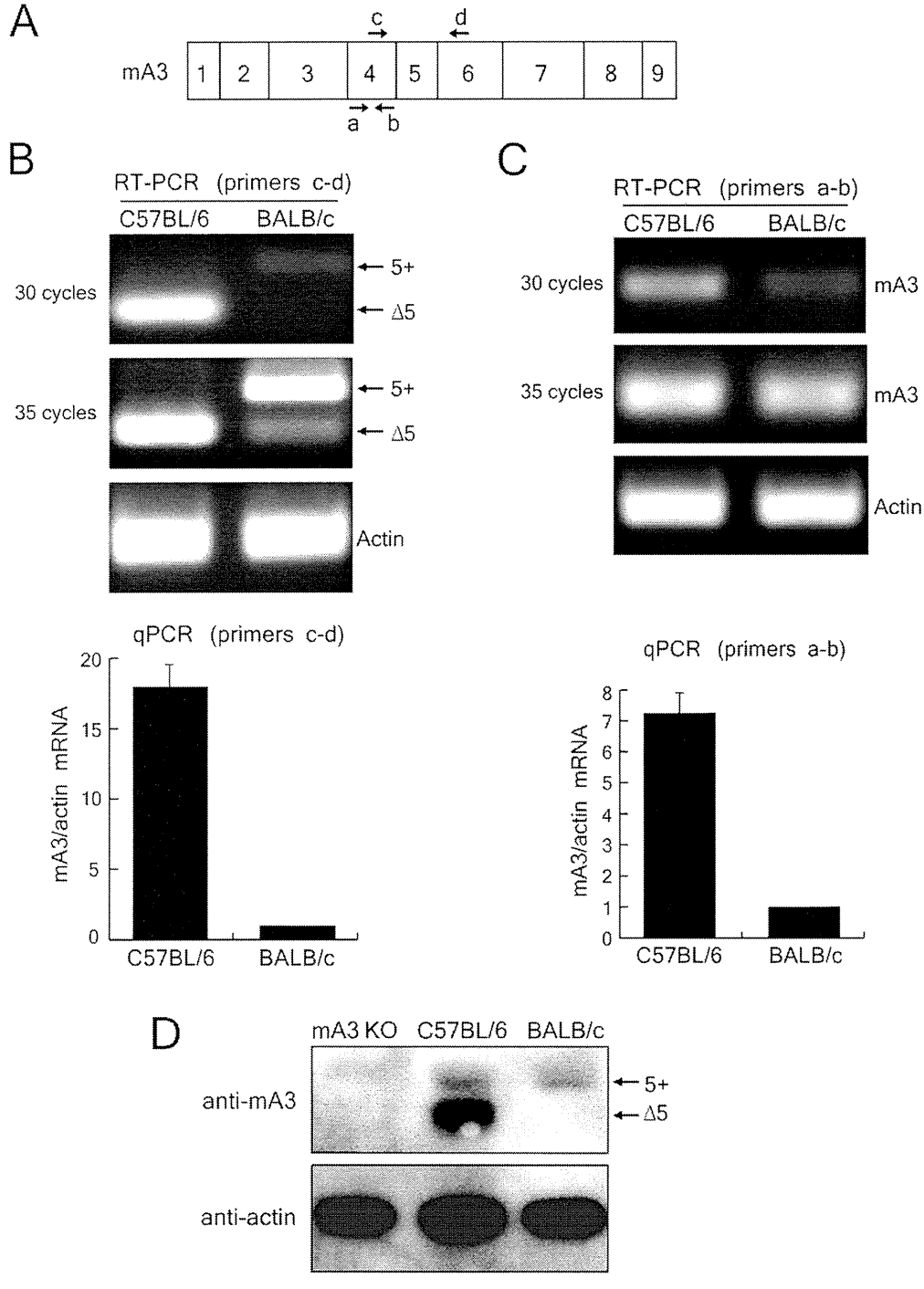

Figure 1. Expression of mA3 transcripts and protein in the spleens of B6 and BALB/c mice. (A) Schematic representation of the mouse APOBEC3 exon composition. The exons are indicated by numbers and their relative sizes are depicted. The arrows indicate the locations of the PCR primers used in the following experiments. (B and C) RT-RCR and quantitative real-time PCR (qPCR) analyses showing splicing patterns and quantities of mA3 mRNA in B6 and BALB/c spleen cells. The primers utilized were c-d for assays shown in (B) and a–b for those in (C). 5+, exon 5-containing mA3; Δ5, mA3 lacking exon 5. Actin was used as an internal control. Quantitative real-time PCR data show averages of three reaction wells and SD. (D) Immunoblot detection of mA3 protein expressed in mouse spleen cells. The spleen cell extracts were tested for their total protein content by Bradford assays and the same amount of protein was loaded in each lane. Anti-mouse APOBEC3 NT antibody reactive with an N-terminal epitope was first pre-absorbed with the spleen lysate prepared from an mA3-knockout (KO) mouse, and was used as the primary antibody. Mouse actin was used as a loading control. Three independent experiments were done for all assays, and the results were consistent with the representative ones shown here.

doi:10.1371/journal.ppat.1002478.g001

expression in the spleens of B6 mice is much higher than that in BALB/c mice.

Effects of exon 5 inclusion on mA3 protein expression

The mA3 expression data shown in Figure 1 indicate that levels of mA3 protein expression roughly correlate with the corresponding transcript levels in mice with different *Apobec3* alleles. However, we previously observed that even when FLAG-tagged mA3 was expressed under the control of the cytomegalovirus (CMV) promoter, the levels of expression of the 5+ mA3 protein tended to be much lower than those of the Δ5 protein, despite similar levels of mRNA expression in transfected cells [27]. This implies that exon 5 might affect either the efficiency of mA3 translation or protein stability. To evaluate these possibilities, 5+ and Δ5 mA3 expression plasmids were constructed with either B6- or BALB/c-derived mA3 cDNA (Figure 2A). The mA3 cDNA were fused with a FLAG tag at their N-terminus and the transcription was driven by the CMV promoter. After transfection of 293T cells with either one of the FLAG-tagged expression constructs, we quantified mA3 transcripts by qPCR and mA3 protein by immunoblotting (Figure 2, B–D). Based on the co-expressed luciferase activities, similar transfection efficiencies for the 5+ and Δ5 plasmids were confirmed, and the data from the qPCR showed that the 5+ mA3 transcript was more highly expressed than the Δ5 mRNA for both alleles. Nevertheless, the expression levels of the 5+ mA3 protein were lower compared to those of the Δ5 counterpart regardless of the allelic differences, although B6 Δ5 protein was expressed more abundantly than BALB/c Δ5 (Figure 2, B and C). These results indicate that the inclusion of exon 5 does not compromise mA3 mRNA expression, but decreases the steady-state levels of mA3 proteins for both allelic variants.

Exon 5 inclusion does not affect mA3 protein stability but influences its translation

As higher mRNA levels of the 5+ mA3 resulted in lower protein levels in comparison with those for the Δ5 isoform in transfected cells, we next examined the steps at which the synthesis or degradation of mA3 protein was affected by the presence of exon 5. To this end, we transfected 293T cells with an expression plasmid harboring the 5+ or Δ5 mA3 cDNA, and cycloheximide was added to stop protein synthesis. The inhibitor of nuclear factor-κB, IκBα, was utilized as a control, as this protein is known to be in the process of constant degradation and regeneration under serum-containing culture conditions [41]. As expected, immunodetectable IκBα decreased upon cycloheximide treatment, while the solvent alone did not affect the protein content (Figure 3A). On the other hand, mA3 expressed in the same cells did not exhibit any reduction upon cycloheximide treatment regardless of the presence or absence of exon 5. Further, the Δ5 protein was again detected at higher levels than the 5+ protein. These results support the conclusion that the effect of exon 5 inclusion in reducing the amount of expressed mA3 protein is not due to accelerated protein degradation.

We next utilized an *in vitro* transcription and translation procedure to determine if exon 5 affects the translation of mA3 (Figure 3B). When the 5+ or Δ5 mA3 templates were added to the *in vitro* transcription and translation reaction, similar amounts of each transcript were detected by RT-PCR assays both at 30 min and 60 min after the beginning of incubation. However, the tempos of appearance and amounts of the 5+ mA3 protein were different from those of the Δ5 counterpart: a large amount of the Δ5 protein was detected at as early as 30 min after the beginning of incubation, while the 5+ mA3 was undetectable at the same time-point. The 5+ mA3 protein became detectable after 60 min of incubation, but its protein level was still markedly lower than that of the Δ5 counterpart. These results collectively indicate that the inclusion of exon 5 modulates the translation efficiency of mA3 rather than its protein degradation.

The TCCT repeat number variation upstream of exon 5 is partially responsible for exon 5 inclusion into the mA3 transcript

As the inclusion of exon 5 is associated with a reduced level of mA3 protein, we next attempted to identify genetic polymorphisms that affect the splicing patterns of mA3 transcripts in terms of exon 5 inclusion. One possible allelic difference in the mouse *Apobec3* locus putatively associated with its splicing patterns is the possible pre-mRNA branch site polymorphisms found in the intron upstream of exon 5: a T/C SNP that lies within a preferred branch site sequence, TA(T/C)CAAC, and TCCT repeat numbers between this and the acceptor site [38]. As described previously [38], the intron 4 of the BALB/c allele contains a tandem repeat of the TCCT sequence near the intron 4/exon 5 boundary, while the B6 allele contains only a single TCCT copy, changing the length of the putative pyrimidine-rich lariat intermediate. The adjacent T/C SNP at position 741 from the first nucleotide of exon 4 is in linkage with the TCCT repeat number. To directly investigate the possible effect of these polymorphisms, we constructed splicing assay plasmids that harbor the *Apobec3* genomic fragment encompassing exons 4 through 7 from either the B6 or BALB/c allele. The resultant plasmids were designated B6 exon 4–7 and BALB exon 4–7 (Figure 4). Three mutants of each of these constructs were made with different combinations of the position 741 T/C SNP and the TCCT copy number variation as depicted in Figure 4B.

Because of the possible presence of species-specific regulatory factors, the resultant genomic constructs were transfected into BALB/3T3 instead of 293T cells along with the luciferase expression plasmid as a control for transfection efficiency. To avoid the amplification of the endogenous mA3 message expressed in BALB/3T3 cells [27], we utilized the primers g and h (Figure 4B) for RT-PCR assays, which were designed to hybridize to the T7 promoter and V5 tag regions of the expression vector. Transfection with the B6 exon 4–7 plasmid resulted in the expression of only the Δ5 transcript, while the BALB exon 4–7 generated both the 5+ and Δ5 transcripts with much higher intensity of the 5+ one (Figure 4C), reproducing the splicing patterns observed in B6 and BALB/c spleens, respectively (Figure 1B). The ratio between the 5+ and Δ5 transcripts was reduced in the samples transfected with BALB ΔTCCT or BALB C741T ΔTCCT plasmid harboring only a single copy of TCCT, which was further confirmed by utilizing the primer i hybridizing to the sequence within exon 5 along with primer h (Figure 4C). Quantitative real-time PCR analyses were done by utilizing another primer (primer j), designed to hybridize with the sequence within exon 5, and further confirmed reduced levels of the exon 5-containing message expressed from the modified BALB exon 4–7 constructs lacking the TCCT repeat. These results imply that the TCCT repeat observed in the BALB/c allele, but not the T/C substitution at position 741, at least partly facilitates the exon 5 inclusion. The lack of an effect of the T/C SNP within the putative branch site sequence was further confirmed by the abundant expression of the 5+ message from the BALB C741T construct. However, both the 5+ and Δ5 transcripts were still produced from the BALB ΔTCCT plasmid, suggesting that the TCCT repeat number is not the only determinant controlling the exon 5 inclusion. In fact, despite the presence of the repeated TCCT, B6 +TCCT and B6 T741C +TCCT did not generate the 5+ message,

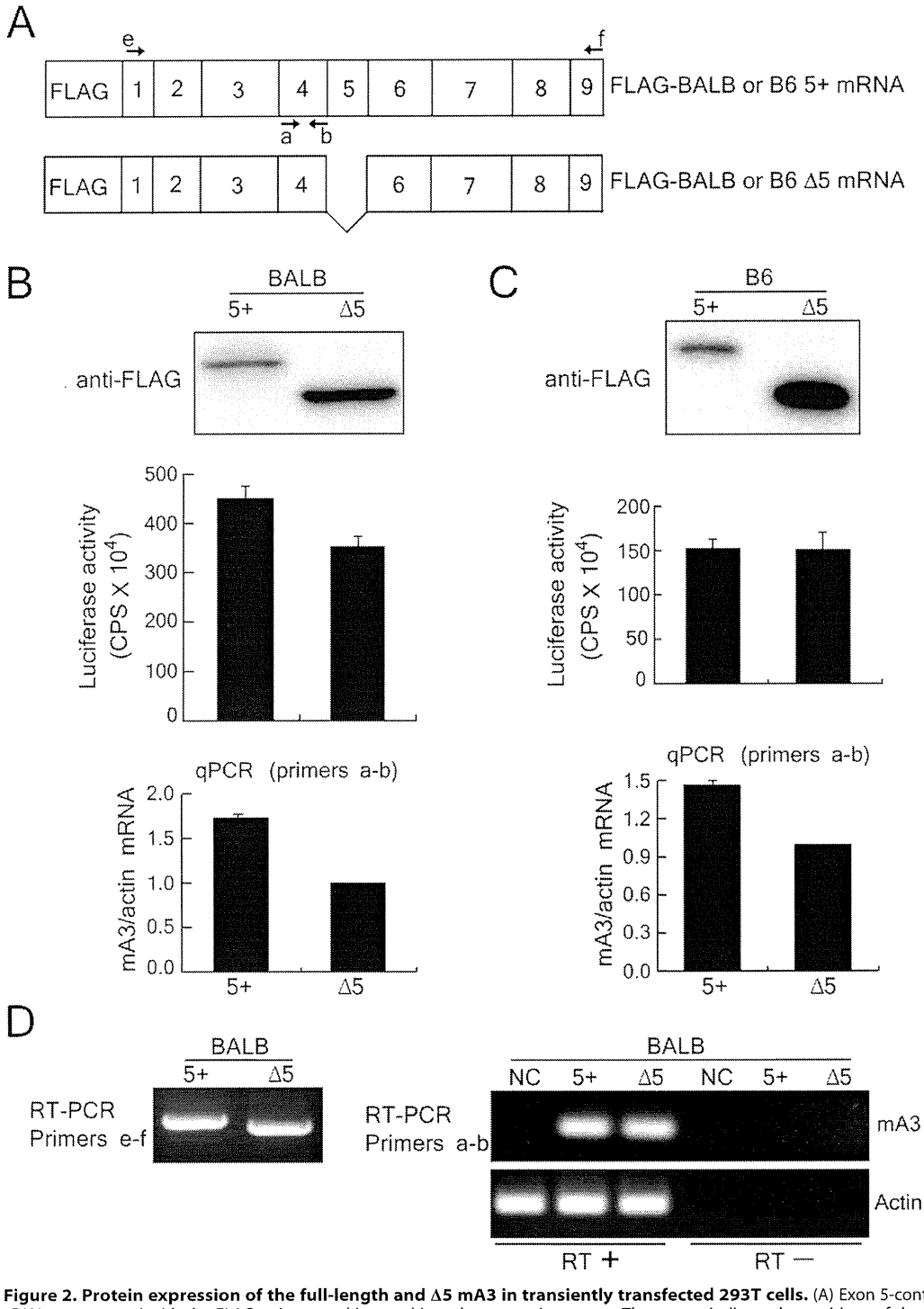

Figure 2. Protein expression of the full-length and Δ5 mA3 in transiently transfected 293T cells. (A) Exon 5-containing (5+) and Δ5 mA3 cDNA were tagged with the FLAG epitope and inserted into the expression vector. The arrows indicate the positions of the PCR primers. The primer set a-b is the same as shown in Figure 1. (B and C) 293T cells were transfected with pFLAG-CMV2-*mA3*^{d} or pFLAG-CMV2-*mA3*^{d}Δ5 in B or with pFLAG-CMV2-*mA3*^{b} or pFLAG-CMV2-*mA3*^{b}Δ5 in C, which express either the 5+ or Δ5 mA3 cDNA cloned from BALB/c or B6 mice, respectively [27]. A luciferase-expressing plasmid, *pluc*, was co-transfected to standardize transfection efficiencies. At 24 hours after transfection, each one-third of the transfected cells was used for immunoblotting, RNA extraction, and luciferase assays. For immunoblotting, the full-length and Δ5 mA3 proteins were detected with the anti-FLAG antibody. Quantitative real-time PCR reactions were carried out with primer set a-b and were normalized with the levels of actin transcripts expressed in 293T cells. Data shown are averages of three reaction wells and SD. (D) RT-PCR assays were performed with (RT+) or without (RT−) reverse transcription to demonstrate specific detection of expected mRNA. Both primer sets e-f and a-b were used to detect mA3 mRNA. NC, negative control transfected with the empty vector, pFLAG-CMV2. RT− samples were included to evaluate the possible contamination of transfected DNA. Specific amplification of cDNA generated in the presence of RT was observed in the cells transfected with a plasmid expressing the 5+ or Δ5 mA3 cDNA. Similar results were obtained for the corresponding B6-derived cDNA clones.
doi:10.1371/journal.ppat.1002478.g002